PAPER

Nondestructive testing of delaminated interfaces between two materials using electromagnetic interrogation

IOP Publishing Inverse Problems

Inverse Problems **34** (2018) 065005 (36pp) https://doi.org/10.1088/1361-6420/aabb1c

Nondestructive testing of delaminated interfaces between two materials using electromagnetic interrogation

Fioralba Cakoni[1], **Irene de Teresa**[2,3] **and Peter Monk**[2]

[1] Mathematics, Rutgers University, Piscataway, NJ 08854-8019, United States of America
[2] Mathematical Sciences, University of Delaware, Newark, DE 19716, United States of America
[3] Structural and Computational Biology, European Molecular Biology Laboratory, Meyerhofstrasse 1, 69117 Heidelberg, Germany

E-mail: fc292@math.rutgers.edu, irene.de.teresa@embl.de and monk@udel.edu

Received 12 October 2017, revised 27 March 2018
Accepted for publication 3 April 2018
Published 27 April 2018

Abstract

We consider the problem of detecting whether two materials that should be in contact have separated or delaminated using electromagnetic radiation. The interface damage is modeled as a thin opening between two materials of different electromagnetic properties. To derive a reconstruction algorithm that focuses on testing for the delamination at the interface between the two materials, we use the approximate asymptotic model for the forward problem derived in de Teresa (2017 *PhD Thesis* University of Delaware). In this model, the differential equations in the small opening are replaced by approximate transmission conditions for the electromagnetic fields across the interface. We also assume that the undamaged or background state is known and it is desired to find where the delamination has opened. We adapt the linear sampling method to this configuration in order to locate the damaged part of the interface from a knowledge of the scattered field and the undamaged configuration, but without needing to know the electromagnetic properties of the opening. Numerical examples are presented to validate our algorithm.

Keywords: nondestructive testing, inverse scattering, screens, Maxwell equations, linear sampling method, asymptotic methods

(Some figures may appear in colour only in the online journal)

1. Introduction

We consider two materials that should have a coincident boundary (in the undamaged or background state), and we wish to detect whether there is a part of the common boundary where the two materials have separated using electromagnetic radiation in the microwave regime. In particular, we want to determine the size and position of the delamination. The applications of this problem include detection of debonding in integrated electric circuits, nondestructive testing of interfaces between two different materials, and potentially the identification of thin biological tissues connected to early stages of cancer development. For a survey on problems in non-destructive testing based on electromagnetic imaging we refer the reader to [14, 19], whereas for some applications to related problems in medical imaging we refer to [17, 29]. This work extends the linear sampling method for detecting delamination using acoustic waves [7] to the electromagnetic case. However, the inherent technical difficulties associated with the analysis of Maxwell's equations have forced us to restrict ourselves to the specific case of the detection of planar delaminations of constant thickness. Related models and other inversion techniques can be found e.g. in [1, 2]. We start by formulating our problem and making the necessary simplifications in order to carry through the analysis of the forward problem derived in [11] to the inverse scattering problem.

1.1. Formulation of the problem

We study the scattering of a time harmonic electromagnetic wave with fixed frequency ω by a layered isotropic penetrable inhomogeneity $\Omega \subset \mathbb{R}^3$, that is schematically depicted in figure 1. We denote by $\Gamma_1 = \partial\Omega$ the boundary of Ω, and by $\Omega_{\text{ext}} := \mathbb{R}^3 \setminus \overline{\Omega}$ the exterior domain. In what follows we assume for simplicity of presentation that Γ is a smooth surface (however as it will become clear later Γ can be piece-wise smooth such that the delaminated part is smooth). In the undamaged or *background* state, we consider Ω to be composed by two layers of different materials, Ω^b_- and Ω^b_+, where Ω^b_- is simply connected and Ω^b_+ is connected. The boundary of Ω^b_-, denoted by Γ, is the common interface of the two layers Ω^b_- and Ω^b_+, and it is an orientable $\mathcal{C}^2$ regular surface (see figure 1, panel (a)).

In the damaged or *defective* state, the two layers have separated and the thin delamination Ω_δ has appeared (the parameter δ will measure the thickness of the delamination and is assumed to be small compared to the wavelength of the radiation in Ω_{ext}). The section $\Gamma_0 := \Gamma \cap \Omega_\delta$ is precisely where the original layers have separated. In this defective configuration $\Omega = \text{int}(\overline{\Omega_+ \cup \Omega_- \cup \Omega_\delta})$. We will assume throughout this paper that Γ_0 is an open surface with Lipschitz continuous relative boundary $\partial\Gamma_0$. It will also be assumed that Γ_0 lies on a planar section of Γ, and that Ω_δ is a cylinder having constant thickness formed by translating Γ_0 normal to the planar surface (see figures 1 and 2).

The four different domains, Ω_{ext}, Ω_+, Ω_- and Ω_δ, indicate the supports of different linear isotropic materials characterized by their electric permittivity $\widehat{\epsilon} > 0$, conductivity $\widehat{\sigma} \geqslant 0$ and magnetic permeability $\widehat{\mu} > 0$. The homogeneous exterior domain Ω_{ext} has constant material properties denoted by $\widehat{\epsilon}_0$, $\widehat{\sigma}_0 = 0$, and $\widehat{\mu}_0$, respectively. For the purposes of this work, it will be useful to define the relative electric permittivity and relative magnetic permeability μ by (see [21])

$$\epsilon = \frac{1}{\widehat{\epsilon}_0}\left(\widehat{\epsilon} + \frac{\mathrm{i}\widehat{\sigma}}{\omega}\right) \quad \text{and} \quad \mu = \frac{\widehat{\mu}}{\widehat{\mu}_0},$$

so that $\epsilon = \mu = 1$ in Ω_{ext}, and both parameters in the other three sub-domains, Ω_+, Ω_- and Ω_δ, are denoted by:

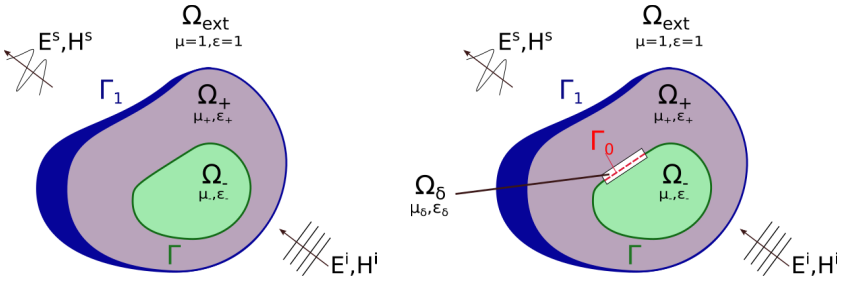

Figure 1. Panel (a): cross section of the undamaged state. Panel (b): cross section of the damaged or defective obstacle. The thin domain Ω_δ represents the delamination.

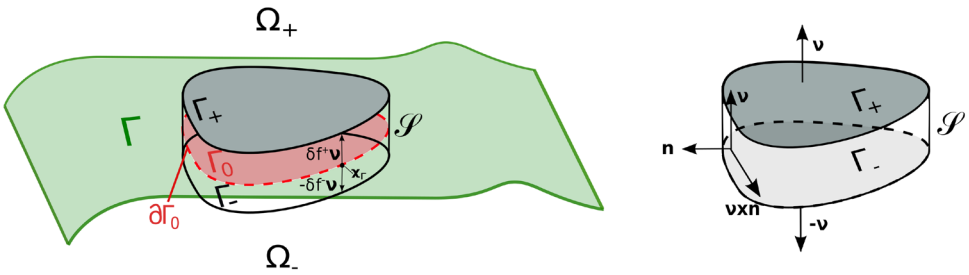

Figure 2. Details of the delamination and corresponding notation. Left: a zoom on the planar thin domain Ω_δ showing Γ and Γ_0. Right: normal vectors on the boundary of the thin domain Ω_δ.

$$\mu = \begin{cases} \mu_+ & \text{in} \quad \Omega_+ \\ \mu_- & \text{in} \quad \Omega_- \\ \mu_\delta & \text{in} \quad \Omega_\delta \end{cases} \quad \text{and} \quad \epsilon = \begin{cases} \epsilon_+ & \text{in} \quad \Omega_+ \\ \epsilon_- & \text{in} \quad \Omega_- \\ \epsilon_\delta & \text{in} \quad \Omega_\delta \end{cases}$$

respectively. Throughout this paper we assume that material properties satisfy:

Assumption 1.1 (On the material properties).

- The functions $\mu : \overline{\Omega} \to \mathbb{R}$ and $\epsilon : \overline{\Omega} \to \mathbb{C}$ are piece-wise smooth. Moreover, $\Re(\epsilon) > 0$, $\Im(\epsilon) \geqslant 0$, and $0 < \mu^{-1} < C$ for some constant $C > 0$.
- *The material properties in the thin delamination, μ_δ and ϵ_δ, are constant.*
- *There is an open neighborhood $\mathcal{N}$ of Ω_δ where the functions $\mu_\pm$ and $\epsilon_\pm$, are constant.*

The assumptions on the cylindrical geometry of the thin delamination Ω_δ, imply that its boundary $\partial\Omega_\delta$ may be split into three different regular surfaces (see figure 2): the two flat parallel faces denoted by Γ_+ and Γ_-, and the tubular side denoted by $\mathscr{S}$. Thus $\overline{\partial\Omega_\delta} = \overline{\Gamma_+ \cup \Gamma_- \cup \mathscr{S}}$. We denote by $\boldsymbol{\nu}$ the unit normal vector on Γ_1 pointing towards Ω_{ext}, and on $\Gamma \setminus \overline{\Gamma_0}$ towards Ω_+, and by $\mathbf{n}$ the normal on $\mathscr{S}$ pointing out of Ω_δ (see figure 2).

Recalling the definition of the relative material properties 1, we can define as it is customarily done in mathematical literature (see [10, 21]), the total electric and magnetic fields by $\mathbf{E} = \sqrt{\epsilon_0}\,\widehat{\mathcal{E}}$ and $\mathbf{H} = \sqrt{\mu_0}\,\widehat{\mathcal{H}}$, respectively, where $\widehat{\mathcal{E}}(x,t) = 1/\sqrt{\epsilon_0}E(x)\mathrm{e}^{\mathrm{i}k\omega}$ and $\widehat{\mathcal{H}}(x,t) = 1/\sqrt{\mu_0}H(x)\mathrm{e}^{\mathrm{i}k\omega}$ and ω is the frequency. Letting $k = \omega\sqrt{\epsilon_0\mu_0}$ denote the positive wave number, we may write the equations that model the scattering of the time harmonic total electromagnetic fields as

$$\nabla \times \mathbf{H} + \mathrm{i}k\epsilon\mathbf{E} = \mathbf{0} \quad \text{and} \quad \nabla \times \mathbf{E} - \mathrm{i}k\mu\mathbf{H} = \mathbf{0} \quad \text{in} \quad \Omega_+ \cup \Omega_\delta \cup \Omega_- \cup \Omega_{\text{ext}}, \tag{1}$$

where we have assumed that there is no applied current. Across the interfaces Γ_1, $\Gamma_\pm$, $\mathscr{S}$, and $\Gamma\backslash\overline{\Gamma}_0$ both $\boldsymbol{\nu} \times \mathbf{H}$ and $\boldsymbol{\nu} \times \mathbf{E}$ are assumed to be continuous.In the unbounded domain Ω_{ext} the total fields can be decomposed as $\mathbf{E} = \mathbf{E}^s + \mathbf{E}^i$ and $\mathbf{H} = \mathbf{H}^s + \mathbf{H}^i$, where $(\mathbf{E}^i, \mathbf{H}^i)$ denote the incident fields which are entire solutions to (1) with $\epsilon = \mu = 1$, and $(\mathbf{E}^s, \mathbf{H}^s)$ are the radiating fields that satisfy the Silver–Müller radiation condition:

$$\lim_{r\to\infty} r\,(\mathbf{H}^s \times \widehat{\mathbf{x}} - \mathbf{E}^s) = \mathbf{0}, \tag{2}$$

where $\widehat{\mathbf{x}} = \frac{\mathbf{x}}{|\mathbf{x}|}$, $r = |\mathbf{x}|$, and the convergence is uniform in all directions $\widehat{\mathbf{x}} \in \mathbb{S}^2$.

Following the ideas in [7, 13, 18, 25] we will substitute the full model (1) and (2) by an asymptotic model, where instead of solving the differential equations in Ω_δ, we replace it by appropriate approximate transmission conditions (ATCs) of the fields in Ω_+ and Ω_-, across the two boundaries Γ_+ and Γ_- with expressions defined on the delaminated portion Γ_0. From the inverse problem perspective this allows for accurate testing of the interface in order to detect the damage.

The paper is organized as follows. In the next section we sketch the derivation of the ATCs model, setup the analytical framework and recall the necessary well-posedeness results from [11] for the ATCs model of the direct scattering problem. Section 3 is dedicated to the study of the inverse problem which is the main goal of this paper. In particular, we prove a mixed reciprocity result which helps us dealing with the inhomogeneous background and develop a modified version of the linear sampling method which enable us to efficiently test along the interface Γ to detect the delaminated part Γ_0. Finally, in section 4, we present two numerical examples showing the viability of our imaging method.

2. Asymptotic model for the forward problem

The approximate model proposed here that arises from substituting the differential equations in Ω_δ with the ATCs, belongs to the family *Chun's*-type models (see [9, 16]). In *Chun's*-type models, the ATCs are expressed in terms of jumps of traces of functions *across two different surfaces*, as opposed to the *crack*-type models used for example in [7], where the ATCs are expressed in terms of jumps of traces *on the same surface* referred to as the crack. It is important to mention here that the *crack*-type ATCs model for electromagnetic scattering (similar to the one proposed in [7]), leads to a variational formulation where well-posedness results are difficult to prove due to incompatibility of signs between the terms involved. In fact, the associated time-domain model has already been discussed in [9], and it has been proven there that in general there are no energy bounds for the corresponding solutions. For the reasons mentioned above, the ATCs model that we use in the current work considers the jumps and average values among traces of the fields on the two different surfaces Γ_- and Γ_+. We recall here the model discussed in [11] for flat delaminations. A more complete derivation of our asymptotic model can be found in [11].

Let us start with setting up some important definition of the surface differential operators. To this end, it is known that at each $\mathbf{x}'_\Gamma$ on smooth open subset of Γ there exists an open neighborhood $U \subset \Gamma$ of $\mathbf{x}'_\Gamma$ where a local parametrization (i.e. homeomorphism) $\boldsymbol{\xi} = (\xi_1, \xi_2) \mapsto \mathbf{x}_\Gamma$ is well defined [15], and which without loss of generality induces a positive orientation of Γ, consistent with the pointing direction of $\boldsymbol{\nu}$. For flat parts this is the obvious rigid transformation. Let $0 < \eta_*$ be a real number such that in the open neighborhood of Γ given by

$$\mathcal{N} := \{\mathbf{x} \in \mathbb{R}^3 \mid \min_{\mathbf{y}\in\Gamma} |\mathbf{x} - \mathbf{y}| < \eta_*\}, \tag{3}$$

the mapping

$$(\mathbf{x}_\Gamma, \eta) \mapsto \mathbf{x} = \mathbf{x}_\Gamma + \eta \boldsymbol{\nu}(\mathbf{x}_\Gamma),$$

is an isomorphism. Moreover, define the vector field $\breve{\boldsymbol{\nu}}$ in $\mathcal{N}$ by

$$\breve{\boldsymbol{\nu}}(\mathbf{x}_\Gamma + s\boldsymbol{\nu}) := \boldsymbol{\nu}(\mathbf{x}_\Gamma), \text{ for all } \mathbf{x}_\Gamma \in \Gamma \text{ and } |\eta| < \eta_*,$$

then the curvature tensor defined by $\mathcal{C}_{\mathbf{x}_\Gamma} := \nabla_\Gamma \breve{\boldsymbol{\nu}}(\mathbf{x}_\Gamma)$ is identically zero for all $\mathbf{x}_\Gamma$ on Γ_0. The tangential vectors $\{\boldsymbol{\tau}_\alpha := \partial_{\xi_\alpha} \mathbf{x}_\Gamma\}_{\alpha=1,2}$ are called the covariant basis of the tangent plane $T_{\mathbf{x}_\Gamma}$ to Γ at $\mathbf{x}_\Gamma$.

Let $\mathbf{v}$ be a $\mathcal{C}^\infty(\Gamma_0)^3$ vector field, then we define the tangential and normal projection of $\mathbf{v}$, respectively, by:

$$\Pi_{||}\mathbf{v} = \boldsymbol{\nu} \times (\mathbf{v} \times \boldsymbol{\nu}) \quad \text{and} \quad \Pi_N \mathbf{v} = \boldsymbol{\nu} \cdot \mathbf{v}. \tag{4}$$

Using compact notation, the tangential and normal projections on Γ_0 will be denoted by $\mathbf{v}_T := (\boldsymbol{\nu} \times \mathbf{v}) \times \boldsymbol{\nu}$ and $\mathbf{v}_N := \boldsymbol{\nu} \cdot \mathbf{v}$, respectively. Analogously, for the parallel surfaces $\Gamma_\pm$ to Γ_0, if $\mathbf{v}^\pm$ are in $\mathcal{C}^\infty(\Gamma_\pm)^3$, then we write for short their respective tangential and normal projections on $\Gamma_\pm$ as: $\mathbf{v}_T^\pm := (\boldsymbol{\nu} \times \mathbf{v}^\pm) \times \boldsymbol{\nu}$ and $\mathbf{v}_N^\pm := \boldsymbol{\nu} \cdot \mathbf{v}^\pm$.

Remark 2.1. It is well known that the projections $\Pi_{||}$ and Π_N defined by (4) have continuous extensions $\gamma_T^\pm : \mathbf{H}(\text{curl}, \mathcal{N} \cap \Omega_\pm) \to \mathbf{H}^{-1/2}(\text{curl}_\Gamma, \Gamma_0)$ and $\gamma_N^\pm : \mathbf{H}(\text{div}, \mathcal{N} \cap \Omega_\pm) \to H^{-1/2}(\Gamma_0)$, respectively (see [21]).

Given a sufficiently smooth scalar field u defined on Γ_0, its surface gradient is given by

$$\nabla_\Gamma u(\mathbf{x}_\Gamma) := \nabla \breve{u}(\mathbf{x}_\Gamma),$$

where the scalar field $\breve{u} : \mathcal{N} \to \mathbb{C}$ is defined by $\breve{u}(\mathbf{x}_\Gamma + \eta \boldsymbol{\nu}(\mathbf{x}_\Gamma)) := u(\mathbf{x}_\Gamma)$. In terms of the covariant basis $\{\boldsymbol{\tau}_\alpha\}$, it can be written as $\nabla_\Gamma = (\partial_{\xi_1} \cdot)\boldsymbol{\tau}_1 + (\partial_{\xi_2} \cdot)\boldsymbol{\tau}_2$. By definition, the adjoint operator of ∇_Γ is $-\text{div}_\Gamma$, which for all smooth vector fields $\mathbf{v}$ defined on Γ_0 satisfies $\text{div}_\Gamma \mathbf{v} = \partial_{\xi_1}(\mathbf{v} \cdot \boldsymbol{\tau}_1) + \partial_{\xi_2}(\mathbf{v} \cdot \boldsymbol{\tau}_2)$.

Important surface differential operators for the upcoming analysis, will be the scalar and vectorial surface curl operators, respectively denoted by curl_Γ and $\overrightarrow{\text{curl}}_\Gamma$, defined as follows: given a smooth tangential vector $\boldsymbol{\eta} = \eta_1 \boldsymbol{\tau}_1 + \eta_2 \boldsymbol{\tau}_2 \in (\mathcal{C}^\infty(\Gamma_0))^3$ and a smooth scalar field $\rho \in \mathcal{C}^\infty(\Gamma_0)$,

$$\text{curl}_\Gamma \boldsymbol{\eta} := \partial_1 \eta_2 - \partial_2 \eta_1 \quad \text{and} \quad \overrightarrow{\text{curl}}_\Gamma \rho := \partial_2 \rho \boldsymbol{\tau}_1 - \partial_1 \rho \boldsymbol{\tau}_2.$$

Now we are ready to formulate the *approximate transmission conditions* (ATCs). To this end we assume that the thin delamination is such that $\overline{\Omega}_\delta \subset \mathcal{N}$ (where $\mathcal{N}$ is defined by (3)), then, as shown in figure 2, the two boundaries $\Gamma_\pm$ of Ω_δ can be written in our new curvilinear coordinates as follows:

$$\Gamma_\pm := \left\{ \mathbf{x}_{\Gamma_\pm} = \mathbf{x}_\Gamma \pm \delta f^\pm \boldsymbol{\nu} \,:\, \mathbf{x}_\Gamma \in \Gamma_0 \right\},$$

where $0 < \delta \ll 1$ is the thickness of the thin delamination and $f^+, f^- \geqslant 0$ are constants such that $f^+ + f^- = 1$. For a given function u (either scalar or vectorial) whose traces are well-defined on Γ_+ and Γ_-, and letting $u^+ := u$ in Ω_+ and $u^- = u$ in Ω_-, we denote the jump and average value of u by:

$$[\![u]\!] = u^+|_{\Gamma_+} - u^-|_{\Gamma_-} \qquad \text{and} \qquad \langle\!\langle u \rangle\!\rangle = \frac{1}{2}(u^+|_{\Gamma_+} + u^-|_{\Gamma_-}).$$

It can be shown after some calculations (see proposition C.3.1 in [11]), that under the hypothesis of a planar thin domain of constant thickness, ATCs of the second order in δ are

$$[\![\boldsymbol{\nu}\times\mathbf{E}]\!] = \mathrm{i}k\delta\alpha_1\langle\!\langle\mathbf{H}_T\rangle\!\rangle - \mathrm{i}k\delta\beta_1\overrightarrow{\mathrm{curl}}_\Gamma\,\mathrm{curl}_\Gamma\langle\!\langle\mathbf{H}_T\rangle\!\rangle \quad \text{on} \quad \Gamma_0, \tag{5}$$

$$[\![\boldsymbol{\nu}\times\mathbf{H}]\!] = \frac{1}{\mathrm{i}k}\delta\alpha_2\langle\!\langle\mathbf{E}_T\rangle\!\rangle - \frac{1}{\mathrm{i}k}\delta\beta_2\overrightarrow{\mathrm{curl}}_\Gamma\,\mathrm{curl}_\Gamma\langle\!\langle\mathbf{E}_T\rangle\!\rangle \quad \text{on} \quad \Gamma_0, \tag{6}$$

and $\alpha_1 = 2\mu_\delta$, $\alpha_2 = 2k^2\epsilon_\delta$, $\beta_1 = \frac{2}{k^2\epsilon_\delta}$, and $\beta_2 = \frac{2}{\mu_\delta}$. Note that for our model in general the second order terms become very complicated hence stopped our calculations at the first order. However in the special case when Γ_0 is the mid-surface between Γ^+ and Γ^- higher order terms are derived in [9]. Also notice that our ATC's for flat surface depends only on the material properties and the thickness of the opening. For general curved opening, the ATC's also involve geometrical features of the surface (see [11]). Because the delamination does not cover the whole boundary Γ we also need a boundary condition on $\mathscr{S}$. We assume that

$$\mathbf{n}\times\mathbf{H} = \mathbf{0} \text{ on } \mathscr{S}. \tag{7}$$

This condition is *ad hoc* and not derived by asymptotic analysis (it is based on the intuitive vanishing flux condition that would correspond to the acoustic model), nevertheless it is essential to our analysis. It is sufficient, however, to obtain a well posed problem. Therefore the second order ATCs model that we base our inversion algorithm consists of equations (1) in the domains $\Omega_-\cup\Omega_+\cup\Omega_{\mathrm{ext}}$, and the transmission conditions (5) and (6). For numerical validation of this model see [11].

In terms of only the electric field $\mathbf{E}$ the ATCs model gives rise to the problem: Find $\mathbf{E}\in\mathbf{H}(\mathrm{curl},\mathbb{R}^3\setminus\overline{\Omega}_\delta)$ satisfying

$$\nabla\times\left(\mu^{-1}\nabla\times\mathbf{E}\right) - k^2\epsilon\mathbf{E} = \mathbf{0} \quad \text{in} \quad \Omega_+\cup\Omega_-\cup\Omega_{\mathrm{ext}}, \tag{8}$$

$$[\![\boldsymbol{\nu}\times\mathbf{E}]\!] = \delta\alpha_1\langle\!\langle\left(\mu^{-1}\nabla\times\mathbf{E}\right)_T\rangle\!\rangle - \delta\beta_1\overrightarrow{\mathrm{curl}}_\Gamma\,\mathrm{curl}_\Gamma\langle\!\langle\left(\mu^{-1}\nabla\times\mathbf{E}\right)_T\rangle\!\rangle \text{ on } \Gamma_0, \tag{9}$$

$$[\![\boldsymbol{\nu}\times\left(\mu^{-1}\nabla\times\mathbf{E}\right)]\!] = \delta\alpha_2\langle\!\langle\mathbf{E}_T\rangle\!\rangle - \delta\beta_2\overrightarrow{\mathrm{curl}}_\Gamma\,\mathrm{curl}_\Gamma\langle\!\langle\mathbf{E}_T\rangle\!\rangle \text{ on } \Gamma_0, \tag{10}$$

$$\mathbf{n}\times\left(\mu^{-1}\nabla\times\mathbf{E}\right) = \mathbf{0} \text{ on } \mathscr{S}, \tag{11}$$

where, in Ω_{ext}, $\mathbf{E} = \mathbf{E}^s + \mathbf{E}^i$ is the total field, $\mathbf{E}^i$ is the incident field, and the scattered field $\mathbf{E}^s$ satisfies the Silver–Müller radiation condition

$$\lim_{r\to\infty} r\left((\nabla\times\mathbf{E}^s)\times\hat{\mathbf{x}} - \mathrm{i}k\mathbf{E}^s\right) = \mathbf{0}, \qquad \text{as } r = |\mathbf{x}|\to+\infty. \tag{12}$$

2.1. The well-posedness of the ATC's model

The complete analysis of the ATC's model of the direct scattering problem is done in [11]. We state the main well-posedness results since it plays an essential role in the analysis of the inverse problem. To this end, we recall the following surface Sobolev spaces (see [20, 21]). If D_Γ denotes either the surface divergence div_Γ or the surface scalar curl_Γ defined in the previous section, then

$$\mathbf{H}^s(D_\Gamma,\Gamma_0) := \{\mathbf{u}\in\mathbf{H}^s(\Gamma_0)\,|\,\boldsymbol{\nu}\cdot\mathbf{u} = 0, \text{ and } D_\Gamma\mathbf{u}\in H^s(\Gamma_0)\},$$

with the graph norm $\|\mathbf{u}\|^2_{\mathbf{H}^s(D_\Gamma,\Gamma_0)} = \|\mathbf{u}\|^2_{\mathbf{H}^s(\Gamma_0)} + \|D_\Gamma \mathbf{u}\|^2_{H^s(\Gamma_0)}$. Let $s \in \mathbb{R}$, then we define

$$\widetilde{\mathbf{H}}^s(D_\Gamma,\Gamma_0) := \{\mathbf{u} \in \widetilde{H}^s(\Gamma_0)^3 \,|\, \boldsymbol{\nu}\cdot\mathbf{u} = 0 \text{ and } D_\Gamma \mathbf{u} \in \widetilde{H}^s(\Gamma_0)\},$$

endowed with the $\mathbf{H}^s(D_\Gamma,\Gamma_0)$ norm, where $\widetilde{H}^s(\Gamma_0)$ are defined by

$$\widetilde{H}^s(\Gamma_0) = \{u \in H^s(\Gamma_0) \,|\, \text{the extension by zero of } u \text{ in } \Gamma,\ \widetilde{u},\ \text{is in } H^s(\Gamma)\},$$

endowed with the restricted $H^s(\Gamma_0)$ inner product. It has been proven (see e.g. [20]) that for $s = 2\ell + 1/2$, $\ell \in \mathbb{Z}$, the space $\widetilde{H}^s(\Gamma_0)$ is precisely the dual space of $H^{-s}(\Gamma_0)$, with respect to the duality pairing

$$\langle v, u\rangle_{H^{-s}(\Gamma_0),\widetilde{H}^s(\Gamma_0)} := \langle v, \widetilde{u}\rangle_{H^{-s}(\Gamma),H^s(\Gamma)}, \tag{13}$$

where on the right-hand-side of (13) $\widetilde{u}$ is the extension by zero of u to Γ.

Let B_R be an arbitrary ball of radius $R > 0$ that contains the obstacle $\overline{\Omega}$, and denote by S_R its boundary. Multiplying equation (8) by a test function $\mathbf{v} \in \mathcal{C}_0^\infty(\mathbb{R}^3)$ and integrating by parts in B_R we obtain

$$\begin{aligned}
&\int_{B_R^\delta} \mu^{-1}\nabla\times\mathbf{E}\cdot\nabla\times\overline{\mathbf{v}} - k^2\epsilon\mathbf{E}\cdot\overline{\mathbf{v}}\ \mathrm{d}\mathbf{y}\\
&+ \int_{\Gamma_0} \langle\!\langle \left(\mu^{-1}\nabla\times\mathbf{E}\right)_T\rangle\!\rangle \cdot \overline{[\![\boldsymbol{\nu}\times\mathbf{v}]\!]}\ \mathrm{d}s(\mathbf{y}) - \int_{\Gamma_0} [\![\boldsymbol{\nu}\times\left(\mu^{-1}\nabla\times\mathbf{E}\right)]\!]\cdot\overline{\langle\!\langle\mathbf{v}\rangle\!\rangle_T}\ \mathrm{d}s(\mathbf{y})\\
&+ \mathrm{i}k\langle G_e(\widehat{\mathbf{x}}\times\mathbf{E}),\mathbf{v}_T\rangle_{S_R} = -\int_{S_R}(\widehat{\mathbf{x}}\times\mathbf{E}^i)\cdot\overline{\mathbf{v}}\ \mathrm{d}s(\mathbf{y}) + \mathrm{i}k\langle G_e(\widehat{\mathbf{x}}\times\mathbf{E}^i),\mathbf{v}_T\rangle_{S_R},
\end{aligned} \tag{14}$$

where $B_R^\delta := B_R \setminus \overline{\Omega_\delta}$, $\langle\cdot,\cdot\rangle_{S_R}$ is understood as the duality pairing between $\mathbf{H}^{-1/2}(\mathrm{div}_{S_R},S_R)$ and $\mathbf{H}^{-1/2}(\mathrm{curl}_{S_R},S_R)$, and $G_e : \mathbf{H}^{-1/2}(\mathrm{div}_{S_R},S_R) \to \mathbf{H}^{-1/2}(\mathrm{div}_{S_R},S_R)$ is the well-known exterior electric-to-magnetic Calderón operator (see [10, 21]) defined by $G_e(\boldsymbol{\lambda}) = \widehat{\mathbf{x}}\times\mathbf{H}^s$, where $(\mathbf{E}^s,\mathbf{H}^s)$ satisfy

$$\begin{aligned}
\mathrm{i}k\mathbf{E}^s + \nabla\times\mathbf{H}^s &= \mathbf{0} \quad \text{in } \mathbb{R}^3\setminus\overline{B}_R,\\
\mathrm{i}k\mathbf{H}^s - \nabla\times\mathbf{E}^s &= \mathbf{0} \quad \text{in } \mathbb{R}^3\setminus\overline{B}_R,\\
\widehat{\mathbf{x}}\times\mathbf{E}^s &= \boldsymbol{\lambda} \quad \text{on } S_R,\\
\lim_{r\to\infty} r(\mathbf{H}^s\times\widehat{\mathbf{x}} - \mathbf{E}^s) &= \mathbf{0},
\end{aligned}$$

where again $\widehat{\mathbf{x}} = \frac{\mathbf{x}}{|\mathbf{x}|}$ and $r = |\mathbf{x}|$. For our analysis, we need to define the trace space

$$\mathcal{H}_0(\Gamma_0) := \widetilde{\mathbf{H}}^{-1/2}(\mathrm{curl}_\Gamma,\Gamma_0)\cap\mathbf{H}(\mathrm{curl}_\Gamma,\Gamma_0)$$

equipped with $\mathbf{H}(\mathrm{curl}_\Gamma,\Gamma_0)$, which is obviously a Hilbert space. Let $\mathcal{H}_0(\Gamma_0)^*$ be the dual space of $\mathcal{H}_0(\Gamma_0)$ with respect to the pivot space $L^2(\Gamma_0)^3$. Since the embedding $\mathcal{H}_0(\Gamma_0)\subset\widetilde{\mathbf{H}}^{-1/2}(\mathrm{curl}_\Gamma,\Gamma_0)$ is bounded, $\mathbf{H}^{-1/2}(\mathrm{div}_\Gamma,\Gamma_0)\subset\mathcal{H}_0(\Gamma_0)^*$ is bounded as well. Now, let us define $\mathcal{A}_i$ on $\mathbf{H}(\mathrm{curl}_\Gamma,\Gamma_0)$ by

$$\mathcal{A}_i\mathbf{u} = \alpha_i\mathbf{u} - \beta_i\overrightarrow{\mathrm{curl}}_\Gamma\mathrm{curl}_\Gamma\mathbf{u}, \quad i = 1,\,2.$$

The following proposition is proven in [11] (see proposition 4.3.1).

Proposition 2.1. *The operator $\mathcal{A}_1 : \mathcal{H}_0(\Gamma_0)\to\mathcal{H}_0(\Gamma_0)^*$ is invertible, except for a discrete number of values $\omega = k^2\epsilon_\delta\mu_\delta$.*

We assume for the rest of this paper that ϵ_δ and μ_δ are such that $\mathcal{A}_1 : \mathcal{H}_0(\Gamma_0) \to \mathcal{H}_0(\Gamma_0)^*$ is invertible. Having established conditions for the invertibility of $\mathcal{A}_1$ in proposition 2.1, we can *formally* replace in the transmission conditions

$$\langle\langle(\mu^{-1}\nabla \times \mathbf{E})_T\rangle\rangle = \mathcal{A}_1^{-1}[\![\boldsymbol{\nu} \times \mathbf{E}]\!].$$

Note that $\mathcal{A}_1^{-1}$ gives us a function extendable by zero to the whole boundary in which is in $\mathbf{H}^{-1/2}(\mathrm{curl}_\Gamma, \Gamma)$. Then from (14), we deduce that (8)–(12) can be written in the following variational formulation: Find $\mathbf{E} \in \mathcal{H}_0$ such that

$$a(\mathbf{E}, \mathbf{v}) = \mathcal{L}(\mathbf{v}) \text{ for all } \mathbf{v} \in \mathcal{H}_0,$$

where,

$$a(\mathbf{E}, \mathbf{v}) = a^+(\mathbf{E}, \mathbf{v}) + b(\mathbf{E}, \mathbf{v}) + \mathrm{i}k\langle G_e(\widehat{\mathbf{x}} \times \mathbf{E}), \mathbf{v}_T\rangle_{S_R},$$

with

$$a^+(\mathbf{E}, \mathbf{v}) := \int_{B_R^\delta} \left(\mu^{-1}\nabla \times \mathbf{E} \cdot \overline{\nabla \times \mathbf{v}}\right) \, \mathrm{d}\,\mathbf{y} + \int_{\Gamma_0} \delta\beta_2 \mathrm{curl}_\Gamma \langle\langle \mathbf{E}_T\rangle\rangle \, \overline{\mathrm{curl}_\Gamma \langle\langle \mathbf{v}_T\rangle\rangle} \, \mathrm{d}s(\mathbf{y}) \tag{15}$$

$$\begin{aligned} b(\mathbf{E}, \mathbf{v}) := &- \int_{B_R^\delta} k^2 \epsilon \mathbf{E} \cdot \overline{\mathbf{v}} \, \mathrm{d}\,\mathbf{y} - \int_{\Gamma_0} \delta\alpha_2 \langle\langle \mathbf{E}_T\rangle\rangle \cdot \overline{\langle\langle \mathbf{v}_T\rangle\rangle} \, \mathrm{d}s(\mathbf{y}) \\ &+ \frac{1}{\delta} \int_{\Gamma_0} \mathcal{A}_1^{-1}[\![\boldsymbol{\nu} \times \mathbf{E}]\!] \cdot \overline{[\![\boldsymbol{\nu} \times \mathbf{v}]\!]} \, \mathrm{d}s(\mathbf{y}), \end{aligned} \tag{16}$$

$$\mathcal{L}(\mathbf{v}) = \int_{S_R} (\widehat{\mathbf{x}} \times (\nabla \times \mathbf{E}^i)) \cdot \overline{\mathbf{v}} - \mathrm{i}k\langle G_e(\widehat{\mathbf{x}} \times \mathbf{E}_i), \mathbf{v}_T\rangle_{S_R},$$

where $B_R^\delta := B_R \setminus \overline{\Omega_\delta}$ and the solutions space is

$$\mathcal{H}_0 := \left\{ \mathbf{u} \in \mathbf{H}(\mathrm{curl}, B_R^\delta) \,\middle|\, \langle\langle \mathbf{u}_T\rangle\rangle \in \mathbf{H}(\mathrm{curl}_\Gamma, \Gamma_0) \text{ and } \mathbf{n} \times \left(\mu^{-1}\nabla \times \mathbf{u}\right)\Big|_{\mathscr{S}} = \mathbf{0} \right\}$$

endowed with the norm

$$||\mathbf{u}||^2_{\mathcal{H}_0} := ||\mathbf{u}||^2_{\mathbf{H}(\mathrm{curl}, B_R^\delta)} + ||\langle\langle \mathbf{u}_T\rangle\rangle||^2_{\mathbf{H}(\mathrm{curl}_\Gamma, \Gamma_0)}.$$

The following theorem is proven in [11].

Theorem 2.1. *Assume in addition to assumption 1.1 that there is a constant* $\epsilon_{\min} > 0$ *such that* $\Re(\epsilon_\pm) \geqslant \epsilon_{\min} > 0$*, and that the constant material properties in* Ω_δ *are such that* $\Re(\epsilon_\delta) > 0$*,* $\Im(\epsilon_\delta) > 0$ *and* $\mu_\delta > 0$*. Then the variational problem*

$$a(\mathbf{u}, \mathbf{v}) = \mathcal{L}(\mathbf{v}) \text{ for all } \mathbf{v} \in \mathcal{H}_0, \tag{17}$$

for all $\mathcal{L} \in \mathcal{H}_0^*$ *has a unique solution that continuously depends on* $\mathcal{L}$*.*

Remark 2.2. It is standard to show that theorem 2.1 together with the fact that (17) is equivalent to (8)–(12) (see [21]) implies that the approximate model (8)–(12) for the forward scattering problem has a unique solution depending continuously on the incident field with respect to the norms determined from theorem 2.1.

Remark 2.3. In [11], it has been shown that the asymptotic model (8)–(11) and (12), converges to the full original model (1) as $\delta \to 0$, although the rate of convergence strictly depends on the geometrical parameters.

3. Inverse problem

We now turn our attention to the main goal of this paper, namely to determine the delaminated part Γ_0 of the boundary Γ. To this end we adapt the linear sampling method to our problem to design a fast algorithm which tests the known interface Γ and detects its delaminated parts.

It is well known (see for example [10] or [6]) that the radiating scattered fields $(\mathbf{E}^s, \mathbf{H}^s)$ of (8)–(12) satisfy the following asymptotic expressions

$$\mathbf{E}^s(\mathbf{x}) = \frac{e^{ikr}}{r}\mathbf{E}^\infty(\widehat{\mathbf{x}}) + O\left(\frac{1}{r^2}\right), \quad \mathbf{H}^s(\mathbf{x}) = \frac{e^{ikr}}{r}\mathbf{H}^\infty(\widehat{\mathbf{x}}) + O\left(\frac{1}{r^2}\right) \quad \text{as } r \to \infty,$$

where $r = |\mathbf{x}|$, $\widehat{\mathbf{x}} = \frac{\mathbf{x}}{|\mathbf{x}|}$, and the convergence is uniform in $\widehat{\mathbf{x}}$. The analytic functions $(\mathbf{E}^\infty, \mathbf{H}^\infty)$ defined on the sphere $\mathbb{S}^2$ are referred to as the electric and magnetic far field patterns, respectively, which are shown (see theorem 2.4 in [6]) to have the following expressions

$$\mathbf{E}^\infty(\widehat{\mathbf{x}}) = \frac{ik}{4\pi}\widehat{\mathbf{x}} \times \int_{\Gamma_1} \{(\boldsymbol{\nu}(\mathbf{y}) \times \mathbf{E}^s(\mathbf{y})) + (\boldsymbol{\nu}(\mathbf{y}) \times \mathbf{H}^s(\mathbf{y}) \times \widehat{\mathbf{x}})e^{-ik\widehat{\mathbf{x}}\cdot\mathbf{y}}\}\, ds(\mathbf{y}),$$

$$\mathbf{H}^\infty(\widehat{\mathbf{x}}) = \frac{ik}{4\pi}\widehat{\mathbf{x}} \times \int_{\Gamma_1} \{(\boldsymbol{\nu}(\mathbf{y}) \times \mathbf{H}^s(\mathbf{y})) - (\boldsymbol{\nu}(\mathbf{y}) \times \mathbf{E}^s(\mathbf{y}) \times \widehat{\mathbf{x}})e^{-ik\widehat{\mathbf{x}}\cdot\mathbf{y}}\}\, ds(\mathbf{y}).$$

For our problem, without loss of generality we use electromagnetic plane waves as incident fields. (Note that our linear sampling method can easily be modified to the case of point sources and near field measurements.) In particular, given a direction vector $\widehat{\mathbf{d}} \in \mathbb{S}^2$ and a polarization vector $\mathbf{p} \in \mathbb{R}^3$ the corresponding electromagnetic plane wave $(\mathbf{E}^i_{pl}(\cdot, \widehat{\mathbf{d}}, \mathbf{p}), \mathbf{H}^i_{pl}(\cdot, \widehat{\mathbf{d}}, \mathbf{p}))$ is defined by:

$$\mathbf{E}^i_{pl}(\mathbf{y}, \widehat{\mathbf{d}}, \mathbf{p}) = ik((\widehat{\mathbf{d}} \times \mathbf{p}) \times \widehat{\mathbf{d}})e^{ik\widehat{\mathbf{d}}\cdot\mathbf{y}} \quad \text{and} \quad \mathbf{H}^i_{pl}(\mathbf{y}, \widehat{\mathbf{d}}, \mathbf{p}) = ik(\widehat{\mathbf{d}} \times \mathbf{p})e^{ik\widehat{\mathbf{d}}\cdot\mathbf{y}}. \tag{18}$$

The pair $(\mathbf{E}, \mathbf{H}) := (\mathbf{E}^i_{pl}(\cdot, \widehat{\mathbf{d}}, \mathbf{p}), \mathbf{H}^i_{pl}(\cdot, \widehat{\mathbf{d}}, \mathbf{p}))$ is an entire solution of the homogeneous Maxwell equations

$$\nabla \times \mathbf{H} + ik\mathbf{E} = \mathbf{0} \quad \text{and} \quad \nabla \times \mathbf{E} - ik\mathbf{H} = \mathbf{0} \quad \text{in} \quad \mathbb{R}^3. \tag{19}$$

For such incident fields the far field pattern of the scattered wave of (8)–(12) will depend on the incident direction $\widehat{\mathbf{d}}$ and polarization $\mathbf{p}$. We indicate this dependence by $(\mathbf{E}^\infty(\cdot, \widehat{\mathbf{d}}, \mathbf{p}), \mathbf{H}^\infty(\cdot, \widehat{\mathbf{d}}, \mathbf{p}))$. Note that ($\mathbf{E}^\infty$ and $\mathbf{H}^\infty$) are related and one determines the other.

The *inverse problem* considered here is to determine the portion Γ_0 of the known interface Γ for a knowledge of the electric far field pattern $\mathbf{E}^\infty(\widehat{\mathbf{x}}, \widehat{\mathbf{d}}, \mathbf{p})$ for $\widehat{\mathbf{x}}, \widehat{\mathbf{d}} \in \mathbb{S}^2_0 \subseteq \mathbb{S}^2$, where $\mathbb{S}^2_0$ is an open subset of the unit sphere, three linearly independent polarization $\mathbf{p} \in \mathbb{R}^3$, and the background configuration depicted in figure 1(a), i.e. known $\Omega_\pm$, $\epsilon_\pm$, $\mu_\pm$ and Γ, but without knowing $\epsilon_\delta, \mu_\delta, f^+, f^-$.

3.1. Reciprocity and mixed reciprocity principles

This subsection is dedicated to present the statements of two basic auxiliary tools needed to develop our inversion scheme, namely a mixed reciprocity result for the solution of the background problem and a reciprocity result for the solution of the ATCs model for the forward problem. The proofs of these results are technical and long, thus for sake of clarity of exposition we defer them to appendices A and B.

3.1.1. Mixed reciprocity for the background problem. We will define the solution of the so called *background* problem to be the unique solution $\mathbf{E}_b$ in $\mathbf{H}_{\rm loc}(\mathrm{curl},\mathbb{R}^3)$ such that:

$$\nabla\times\mathbf{E}_b-\mathrm{i}k\mu\mathbf{H}_b=\mathbf{0}\quad\text{in}\quad\mathbb{R}^3\quad\text{and}\quad\nabla\times\mathbf{H}_b+\mathrm{i}k\epsilon\mathbf{E}_b=\mathbf{0}\quad\text{in}\quad\mathbb{R}^3,\tag{20}$$

where, again, $\mathbf{E}_b=\mathbf{E}_b^s+\mathbf{E}^i$ and $\mathbf{H}_b=\mathbf{H}_b^s+\mathbf{H}^i$ in $\Omega_{\rm ext}$, $\mathbf{E}^i$ is the incident field, and $\mathbf{E}_b^s$ is the scattered field that satisfies the Silver–Müller radiation condition (12). Here

$$\mu=\begin{cases}\mu_+ & \text{in}\quad\Omega_+\\ \mu_- & \text{in}\quad\Omega_-\\ 1 & \text{in}\quad\Omega_{\rm ext}\end{cases}\quad\text{and}\quad\epsilon=\begin{cases}\epsilon_+ & \text{in}\quad\Omega_+\\ \epsilon_- & \text{in}\quad\Omega_-\\ 1 & \text{in}\quad\Omega_{\rm ext}.\end{cases}$$

The background solutions are the electric and magnetic fields associated with the undamaged material when the delamination is not present. Note that in the definition of the background problem it is implicit that the tangential components of the electric and magnetic fields are continuous across Γ and Γ_1.

In the particular case of electromagnetic plane wave $(\mathbf{E}^i_{pl}(\cdot,\widehat{\mathbf{d}},\mathbf{p}),\mathbf{H}^i_{pl}(\cdot,\widehat{\mathbf{d}},\mathbf{p}))$, the solution to the background problem (20) is be denoted by $\mathbf{E}_{b,pl}(\cdot,\widehat{\mathbf{d}},\mathbf{p})$ and $\mathbf{H}_b,pl(\cdot,\widehat{\mathbf{d}},\mathbf{p})$, and the corresponding scattered electric field by $\mathbf{E}^s_{b,pl}(\cdot,\widehat{\mathbf{d}},\mathbf{p})\in\mathbf{H}(\mathrm{curl},\mathbb{R}^3\setminus\overline{\Omega})$. Of course the corresponding scattered magnetic field is

$$\mathbf{H}^s_{b,pl}(\cdot,\widehat{\mathbf{d}},\mathbf{p}):=\frac{1}{\mathrm{i}k}\nabla\times\mathbf{E}^s_{b,pl}(\cdot,\widehat{\mathbf{d}},\mathbf{p}).$$

In addition to the plane waves (18), we need another family of radiating solutions to the homogeneous Maxwell equations (19). To this end, for a given vector $\mathbf{p}\in\mathbb{R}^3$, we define the electromagnetic field $(\mathbf{E}^i_{edp}(\cdot,\cdot,\mathbf{p}),\mathbf{H}^i_{edp}(\cdot,\cdot,\mathbf{p}))$ generated by an *electric dipole* with polarization $\mathbf{p}$ by

$$\mathbf{E}^i_{edp}(\mathbf{y},\mathbf{z},\mathbf{p})=-\frac{1}{\mathrm{i}k}\nabla_y\times\nabla_y\times(\mathbf{p}\Phi(\mathbf{y},\mathbf{z}))\quad\text{and}\quad\mathbf{H}^i_{edp}(\mathbf{y},\mathbf{z},\mathbf{p})=\nabla_y\times(\mathbf{p}\Phi(\mathbf{y},\mathbf{z}))$$

where $\Phi(\mathbf{y},\mathbf{z})=\frac{\mathrm{e}^{\mathrm{i}k|\mathbf{y}-\mathbf{z}|}}{4\pi|\mathbf{y}-\mathbf{z}|}$ is the radiating fundamental solution of the Helmholtz equation. It is well known that the electromagnetic pair $(\mathbf{E},\mathbf{H})=(\mathbf{E}^i_{edp}(\cdot,\mathbf{z},\mathbf{p}),\mathbf{H}^i_{edp}(\cdot,\mathbf{z},\mathbf{p}))$ is the radiating fundamental solution of the homogeneous Maxwell equations (see [6]) i.e. it satisfies

$$\nabla\times\mathbf{E}-\mathrm{i}k\mathbf{H}=\mathbf{0}\ \text{in}\quad\text{and}\quad\nabla\times\mathbf{H}+\mathrm{i}k\mathbf{E}=\mathbf{p}\delta(\cdot-\mathbf{z})\qquad\text{in}\ \mathbb{R}^3.$$

Analogously to the incident plane waves, when the incident field is an electric dipole $(\mathbf{E}^i,\mathbf{H}^i):=(\mathbf{E}^i_{b,edp}(\cdot,\cdot,\mathbf{p}),\mathbf{H}^i_{b,edp}(\cdot,\cdot,\mathbf{p}))$, the solution to the background problem (20) is be denoted by $\mathbf{E}_{b,edp}(\cdot,\cdot,\mathbf{p})$ and $\mathbf{H}_{b,edp}(\cdot,\cdot,\mathbf{p})$, and the corresponding scattered electric field by $\mathbf{E}^s_{b,edp}(\cdot,\cdot,\mathbf{p})\in\mathbf{H}(\mathrm{curl},\mathbb{R}^3\setminus\overline{\Omega})$ with the corresponding scattered magnetic field

$$\mathbf{H}^s_{b,edp}(\cdot,\cdot,\mathbf{p}):=\frac{1}{\mathrm{i}k}\nabla\times\mathbf{E}^s_{b,edp}(\cdot,\cdot,\mathbf{p}).$$

Finally, the radiating electromagnetic Green's tensor associated with the background medium is the generalized electric dipole, defined as the pair of second order tensors $(\mathbb{G}^E,\mathbb{G}^H)$ such that for any constant vector $\mathbf{p}\in\mathbb{R}^3$ and $\mathbf{z}\in\mathbb{R}^3$, the corresponding fields $(\mathbb{G}^E(\cdot,\mathbf{z})\mathbf{p},\mathbb{G}^H(\cdot,\mathbf{z})\mathbf{p})\in\mathbf{H}_{\rm loc}(\mathrm{curl},\mathbb{R}^3\setminus\{\mathbf{z}\})\times\mathbf{H}_{\rm loc}(\mathrm{curl},\mathbb{R}^3\setminus\{\mathbf{z}\})$ solve

$$\begin{cases} \nabla_y \times (\mathbb{G}^E(\cdot,\mathbf{z})\mathbf{p}) - \mathrm{i}k\mu\mathbb{G}^H(\cdot,\mathbf{z})\mathbf{p} = \mathbf{0} \text{ in } \mathbb{R}^3, \\ \nabla_y \times (\mathbb{G}^H(\cdot,\mathbf{z})\mathbf{p}) + \mathrm{i}k\epsilon\mathbb{G}^E(\cdot,\mathbf{z})\mathbf{p} = \mathbf{p}\delta(\cdot-\mathbf{z}) \text{ in } \mathbb{R}^3, \\ \lim_{r\to\infty} r((\mathbb{G}^H(\mathbf{x},\mathbf{z})\mathbf{p}) \times \widehat{\mathbf{x}} - \mathrm{i}k\mathbb{G}^E(\mathbf{x},\mathbf{z})\mathbf{p}) = 0. \end{cases} \tag{21}$$

We are now ready to proof a mixed reciprocity principle, similar to those presented in [26] in the electromagnetic case for homogeneous background, and in [5, 7, 8] in the acoustic case for inhomogeneous background.

Theorem 3.1 (Mixed reciprocity principle). *For all* $\widehat{\mathbf{x}} \in \mathbb{S}^2$ *and* $\mathbf{z} \in \mathbb{R}^3 \setminus (\Gamma \cup \Gamma_1)$,

$$4\pi\mathbf{p}\cdot\mathbb{G}^{E,\infty}(\widehat{\mathbf{x}},\mathbf{z})\mathbf{q} = \mathbf{q}\cdot\mathbf{E}_{b,pl}(\mathbf{z},-\widehat{\mathbf{x}},\mathbf{p}), \tag{22}$$

for all $\mathbf{q},\mathbf{p} \in \mathbb{R}^3$. *Moreover, for* $\mathbf{z} \in \Gamma \cup \Gamma_1$ *the identity (22) is true if* $\mathbf{q}\cdot\boldsymbol{\nu}(\mathbf{z}) = 0$ *and* $\mathbf{p}\cdot\boldsymbol{\nu}(\mathbf{z}) = 0$.

3.1.2. Reciprocity for the ATCs model. We now turn our attention to the approximate problem (8)–(12) for the delaminated configuration. We next prove that the reciprocity relation satisfied by far field patterns of solutions to the full model (1) and (2) (see theorem 6.30 in [10]) is still satisfied by far field patterns of radiating solutions to the approximate model. To this end, for the sake of simplicity in the following theorem we denote by $\mathbf{E}^\infty_{pl}(\cdot,\widehat{\mathbf{d}},\mathbf{p})$ and $\mathbf{H}^\infty_{pl}(\cdot,\widehat{\mathbf{d}},\mathbf{p})$ the far field patterns of the radiating solutions $\mathbf{E}^s_{pl}(\cdot,\widehat{\mathbf{d}},\mathbf{p})$ and $\mathbf{H}^s_{pl}(\cdot,\widehat{\mathbf{d}},\mathbf{p})$ to the problem (8)–(12), where of course we have $\mathbf{H}^s_{pl} := -\mathrm{i}k\nabla\times\mathbf{E}^s_{pl}$ in Ω_{ext}.

Theorem 3.2. *(The reciprocity principle for the ATCs model) For all* $\widehat{\mathbf{x}}, d \in \mathbb{S}^2$ *and* $\mathbf{p},\mathbf{q} \in \mathbb{R}^3$,

$$\mathbf{q}\cdot\mathbf{E}^\infty_{pl}(\widehat{\mathbf{x}},\widehat{\mathbf{d}},\mathbf{p}) = \mathbf{p}\cdot\mathbf{E}^\infty_{pl}(-\widehat{\mathbf{d}},-\widehat{\mathbf{x}},\mathbf{q}).$$

We end this section by stating a boundary integral representation formula for the electric field in the case of an inhomogeneous media which is a basic auxiliary tool in the development of the linear sampling method. The proof, which we omit here, is standard and is based on the singularity of the Green's function for the inhomogeneous media and integration by parts formulas.

Remark 3.1 (On the integral representation formula). Let $D \subset \mathbb{R}^3$ be a bounded, simply connected domain with Lipschitz boundary ∂D and denote by ν the unit normal vector on ∂D pointing outwards from D. Let μ and ε be piecewise smooth such that the support of $(\mu-1)$ and $(\epsilon-1)$ is D. Then the radiating scattered field $\mathbf{E}^s \in \mathbf{H}_{\text{loc}}(\text{curl},\mathbb{R}^3)$ corresponding to the incident field $\mathbf{E}^i$ and satisfying

$$\nabla\times(\mu^{-1}\nabla\times\mathbf{E}^s) - k^2\epsilon\mathbf{E}^s = \nabla\times(\mu^{-1}-1)\nabla\times\mathbf{E}^i - k^2(\epsilon-1)\mathbf{E}^i \qquad \text{in } \mathbb{R}^3,$$

has the following representation formula:

$$\mathbf{E}^s(\mathbf{x}) = \frac{1}{\mathrm{i}k}\int_{\partial D}\Big\{-\mu^{-1}(\mathbf{y})\nabla\times\mathbb{G}^E(\mathbf{x},\mathbf{y})\left[\boldsymbol{\nu}\times\mathbf{E}^s\right](\mathbf{y}) + \mathbb{G}^E(\mathbf{x},\mathbf{y})\left[\boldsymbol{\nu}\times(\mu^{-1}(\mathbf{y})\nabla\times\mathbf{E}^s)\right](\mathbf{y}),\Big\}\,\mathrm{d}s(\mathbf{y})$$

$\mathbf{x} \in \mathbb{R}^3 \setminus \partial D$, where $\mathbb{G}^E$ is the electric part of the Green's tensor defined by (21) and $[v] = v^+|_{\partial D} - v^-|_{\partial D}$ denotes the usual jump (see e.g. [22].)

3.2. The linear sampling method

We are now ready to develop a modified linear sampling method to solve the inverse problem formulated at the beginning of this section. For sake of presentation we assume here that $\mathbf{E}^\infty(\widehat{\mathbf{x}}, \widehat{\mathbf{d}}, \mathbf{p})$ is measured for all $\widehat{\mathbf{x}}, \widehat{\mathbf{d}} \in \mathbb{S}^2$. The modification of the linear sampling method for limited aperture is a standard procedure (see e.g. [6]). We start by recalling the *electric Hergoltz wave function* [10]

$$\mathbf{E}_g(\mathbf{x}) = \int_{\mathbb{S}^2} \mathbf{g}(\widehat{\mathbf{d}}) \mathrm{e}^{\mathrm{i}k\mathbf{x}\cdot\widehat{\mathbf{d}}} \ \mathrm{d}s(\widehat{\mathbf{d}}) \qquad \text{for } \mathbf{g} \in \mathbf{L}_t^2(\mathbb{S}^2).$$

The far field operator $\mathcal{F} : \mathbf{L}_t^2(\mathbb{S}^2) \to \mathbf{L}_t^2(\mathbb{S}^2)$ associated with the approximate model of the scattering by the medium with the defect is defined by

$$(\mathcal{F}\mathbf{g})(\widehat{\mathbf{x}}) = \int_{\mathbb{S}^2} \mathbf{E}^\infty(\widehat{\mathbf{x}}, \widehat{\mathbf{d}}, \mathbf{g}(\widehat{\mathbf{d}})) \ \mathrm{d}s(\widehat{\mathbf{d}}),$$

where $\mathbf{E}^\infty(\cdot, \widehat{\mathbf{d}}, \mathbf{g}(\widehat{\mathbf{d}}))$ is the far field pattern of the radiating field $\mathbf{E}^s(\cdot, \widehat{\mathbf{d}}, \mathbf{g}(\widehat{\mathbf{d}}))$ associated with the solution of (8)–(12) when the incident field is the plane wave $\mathbf{E}^i(\cdot, \widehat{\mathbf{d}}, \mathbf{g}(\widehat{\mathbf{d}}))$. By linearity, $\mathcal{F}\mathbf{g}$ is the far field pattern of the radiating solution of (8)–(12) when $\mathbf{E}^i = \mathbf{E}_g$ (see [6]).

In an analogous manner, we can define the far field operator $\mathcal{F}_B : \mathbf{L}_t^2(\mathbb{S}^2) \to \mathbf{L}_t^2(\mathbb{S}^2)$ associated with the background problem (20) by

$$(\mathcal{F}_B\mathbf{g})(\widehat{\mathbf{x}}) = \int_{\mathbb{S}^2} \mathbf{E}_{pl}^\infty(\widehat{\mathbf{x}}, \widehat{\mathbf{d}}, \mathbf{g}(\widehat{\mathbf{d}})) \ \mathrm{d}s(\widehat{\mathbf{d}}),$$

where $\mathbf{E}_{b,pl}^\infty(\cdot, \widehat{\mathbf{d}}, \mathbf{g}(\widehat{\mathbf{d}}))$ is the far field pattern of the radiating field $\mathbf{E}_{b,pl}^s(\cdot, \widehat{\mathbf{d}}, \mathbf{g}(\widehat{\mathbf{d}}))$ solving (20). We denote by $\mathbf{E}_{b,\mathbf{g}}$ and $\mathbf{E}_{b,\mathbf{g}}^s$ the total and radiating field solutions to the background problem (20), respectively, when the incident field is $\mathbf{E}^i = \mathbf{E}_g$. Then, again by linearity, $\mathcal{F}_B\mathbf{g}$ is the far field pattern of $\mathbf{E}_{b,\mathbf{g}}^s$. The far-field operator associated with the defect is now given by

$$\mathcal{F}_D := \mathcal{F} - \mathcal{F}_B,$$

which will provide the information from the scattering by the delamination alone. From our assumption that thebackground state is known $\mathcal{F}_B$ can be computed, whereas $\mathcal{F}$ is what we can measure, then we may develop a method to detect Γ_0 part of Γ based on $\mathcal{F}_D$.

To study the range of $\mathcal{F}_D$ we define the space (of generalized incident fields)

$$\mathcal{H} := \left\{ \mathbf{u} \in \mathbf{H}(\mathrm{curl}, B_R^\delta) \,\middle|\, \mu^{-1}\nabla\times\mathbf{u} \in \mathbf{H}(\mathrm{curl}, B_R^\delta) \text{ and } \langle\langle \mathbf{u}_T \rangle\rangle \in \mathbf{H}(\mathrm{curl}_\Gamma, \Gamma_0) \right\},$$

endowed with its graph norm,

$$\|\mathbf{u}\|_{\mathcal{H}}^2 = ||\mathbf{u}||_{\mathbf{H}(\mathrm{curl}, B_R^\delta)}^2 + ||\mu^{-1}\nabla\times\mathbf{u}||_{L^2(B_R^\delta)}^2 + ||\langle\langle \mathbf{u}_T \rangle\rangle||_{\mathbf{H}(\mathrm{curl}_\Gamma, \Gamma_0)}^2.$$

More generally the *defective* scattering problem for the scattered field $\mathbf{E} \in \mathbf{H}_{\mathrm{loc}}(\mathrm{curl}, \mathbb{R}^3 \setminus \overline{\Omega}_\delta)$ such that $\mathbf{E}|_{B_R^\delta} \in \mathcal{H}$ can be written

$$\begin{cases} \nabla\times\left(\mu^{-1}\nabla\times\mathbf{E}\right) - k^2\epsilon\mathbf{E} = \mathbf{0} & \text{in} \quad \mathbb{R}^3 \setminus \overline{\Omega}_\delta, \\ \mathcal{A}_1^{-1}[\![\boldsymbol{\nu}\times\mathbf{E}]\!] = \delta\langle\langle\left(\left(\mu^{-1}\nabla\times\mathbf{E}\right)_T\right)\rangle\rangle + \mathbf{h}_1 & \text{on} \quad \Gamma_0, \\ [\![\boldsymbol{\nu}\times\left(\mu^{-1}\nabla\times\mathbf{E}\right)]\!] = \delta\mathcal{A}_2\langle\langle\mathbf{E}_T\rangle\rangle + \mathbf{h}_2 & \text{on} \quad \Gamma_0, \\ \mathbf{n}\times\left(\mu^{-1}\nabla\times\mathbf{E}\right) = \mathbf{h}_3 & \text{on} \quad \mathscr{S}, \end{cases} \tag{23}$$

and $\mathbf{E}$ satisfies the Silver–Müller radiation condition (12), where

$$\begin{cases} \mathbf{h}_1 & := & \delta\,\langle\!\langle (\mu^{-1}\nabla\times\mathbf{v})_T\rangle\!\rangle - \mathcal{A}_1^{-1}[\![\boldsymbol{\nu}\times\mathbf{v}]\!], \\ \mathbf{h}_2 & := & \delta\mathcal{A}_2\langle\!\langle \mathbf{v}_T\rangle\!\rangle - [\![\boldsymbol{\nu}\times(\mu^{-1}\nabla\times\mathbf{v})]\!], \\ \mathbf{h}_3 & := & -\mathbf{n}\times\left(\mu^{-1}\nabla\times\mathbf{v}\right)\Big|_{\mathscr{S}}, \end{cases} \tag{24}$$

for some generalized incident field $\mathbf{v}\in\mathcal{H}$. Now, define the *Hergoltz operator* $\mathscr{H}:\mathbf{L}_t^2(\mathbb{S}^2)\to\mathbf{H}(\mathrm{curl}_\Gamma,\Gamma_0)\times\mathcal{H}_0(\Gamma_0)^*\times\mathbf{H}^{-1/2}(\mathrm{div}_{\mathscr{S}},\mathscr{S})$ by

$$\mathscr{H}\mathbf{g}=\Bigg(\delta\langle\!\langle(\mu^{-1}\nabla\times\mathbf{E}_{b,\mathbf{g}})_T\rangle\!\rangle-\mathcal{A}_1^{-1}[\![\boldsymbol{\nu}\times\mathbf{E}_{b,\mathbf{g}}]\!],$$

$$\delta\mathcal{A}_2\langle\!\langle(\mathbf{E}_{b,\mathbf{g}})_T\rangle\!\rangle-[\![\boldsymbol{\nu}\times(\mu^{-1}\nabla\times\mathbf{E}_{b,\mathbf{g}})]\!],-\mathbf{n}\times\left(\mu^{-1}\nabla\times\mathbf{E}_{b,\mathbf{g}}\right)\Big|_{\mathscr{S}}\Bigg),$$

where $\mathcal{A}_i$, $i=1,2$, are the boundary operators defined by (2) and again for a generic vector field $\mathbf{v}$, $\mathbf{v}_T:=(\boldsymbol{\nu}\times\mathbf{v})\times\boldsymbol{\nu}$ denotes the tangent component on the indicated surface.

Remark 3.2. Notice that $\mathcal{F}_D\mathbf{g}$ is, by linearity, the far-field pattern associated with the solution to the defective problem (23) with $\mathbf{E}^i=\mathbf{E}_{b,\mathbf{g}}$, i.e. when the boundary source terms are $\mathscr{H}\mathbf{g}$.

Next we need to define boundary sources to far field solution operator $\mathscr{G}:\mathbf{H}(\mathrm{curl}_\Gamma,\Gamma_0)\times\mathcal{H}_0(\Gamma_0)^*\times\mathbf{H}^{-1/2}(\mathrm{div}_{\mathscr{S}},\mathscr{S})\to\mathbf{L}_t^2(\mathbb{S}^2)$ by

$$\mathscr{G}(\mathbf{h}_1,\mathbf{h}_2,\mathbf{h}_3)=\mathbf{E}^\infty,$$

where $\mathbf{E}^\infty$ is the far field pattern of the scattered field $\mathbf{E}$ that solves the defective problem (23). From theorem 2.1, we know that the operator $\mathscr{G}$ is well defined and bounded.

Then it is clear that the following factorization of the far field operator $\mathcal{F}_D$ holds

$$\mathcal{F}_D=\mathscr{G}\mathscr{H}.$$

Hence in the following we study the properties of $\mathscr{G}$ and $\mathscr{H}$.

Proposition 3.1. *In addition to the assumptions of theorem 2.1, assume that the function* $|\nabla\mu|$ *is piecewise bounded in a neighbourhood of* Γ *and* $\mathbf{n}\times\left(\mu^{-1}\nabla\times\mathbf{E}_{b,\mathbf{g}}\right)\Big|_{\mathscr{S}}=\mathbf{0}$ *if and only if* $\mathbf{g}=\mathbf{0}$. *Then the operator* $\mathscr{H}$ *is injective with dense range.*

The proof of proposition 3.1 can be found in appendix C below.

Remark 3.3. We remark that assumptions of similar type as in proposition 3.1 appear in the study of the injectivity of the Herglotz type operators in the cracks or screen problems and typically do not hold for special symmetric configuration of the scattering problem (see e.g. [6, 7, 30]).

Given a regular surface $L\subset\Gamma$, we define

$$\mathcal{C}_{0,t}^\infty(L):=\left\{\mathbf{u}\in(\mathcal{C}_0^\infty(L))^3\,|\,\boldsymbol{\nu}\cdot\mathbf{u}=0\text{ on }L\right\}.$$

For any density $\mathbf{a}_L\in\mathcal{C}_{0,t}^\infty(L)$, we define ϕ_L^∞ by

$$\boldsymbol{\phi}_L^\infty(\widehat{\mathbf{x}}):=\int_L\mathbb{G}^{E,\infty}(\widehat{\mathbf{x}},\mathbf{y}_\Gamma+\delta f^+\boldsymbol{\nu})\mathbf{a}_L(\mathbf{y}_\Gamma)\;\mathrm{d}\,\mathbf{y}_\Gamma. \tag{25}$$

These $\boldsymbol{\phi}_L^\infty$ are referred to as *test functions*, and are used to characterize the range of $\mathscr{G}$.

Lemma 3.1 (Characterization of the range of $\mathscr{G}$) *Let $L \subset \Gamma$, and $\mathbf{a}_L \in \mathcal{C}^\infty_{0,t}(L)$ such that $\mathbf{a}_L$ does not vanish in any open subset of L. Then $L \subset \Gamma_0$ if and only if $\boldsymbol{\phi}^\infty_L \in Range(\mathscr{G})$.*

Proof. Let $L \subset \Gamma_0$ and $\mathbf{a}_L \in \mathcal{C}^\infty_{0,t}(L)$. Then its extension by zero $\widetilde{\mathbf{a}}_L$ in Γ_0 belongs to $\mathcal{C}^\infty_t(\Gamma_0)$, and the corresponding test function

$$\boldsymbol{\phi}^\infty_L(\widehat{\mathbf{x}}) := \int_L \mathbb{G}^{E,\infty}(\widehat{\mathbf{x}}, \mathbf{y})\mathbf{a}_L(\mathbf{y}) \ \mathrm{d}s(\mathbf{y}) = \int_{\Gamma_0} \mathbb{G}^{E,\infty}(\widehat{\mathbf{x}}, \mathbf{y})\widetilde{\mathbf{a}}_L(\mathbf{y}) \ \mathrm{d}s(\mathbf{y})$$

is the far field pattern of $P\widetilde{\mathbf{a}}_L$, defined by

$$(P\widetilde{\mathbf{a}}_L)(\mathbf{x}) := \begin{cases} \int_{\Gamma_0} \mathbb{G}^E(\mathbf{x}, \mathbf{y}_\Gamma + \delta f^+ \boldsymbol{\nu})\widetilde{\mathbf{a}}_L(\mathbf{y}) \ \mathrm{d}\,\mathbf{y}_\Gamma & \text{in } \mathbb{R}^3 \setminus \overline{\Omega_\delta \cup \Omega_-}, \\ \int_{\Gamma_0} \mathbb{G}^E(\mathbf{x}, \mathbf{y}_\Gamma - \delta f^- \boldsymbol{\nu})\widetilde{\mathbf{a}}_L(\mathbf{y}_\Gamma) \ \mathrm{d}\,\mathbf{y}_\Gamma & \text{in } \Omega_-. \end{cases}$$

Due to well-known properties of the single- and double-layer potentials (see remark 3.1),

$$\begin{aligned} &\nabla \times \mu^{-1}\nabla \times P\widetilde{\mathbf{a}}_L - k^2 \epsilon P\widetilde{\mathbf{a}}_L = \mathbf{0} \quad \text{in } \mathbb{R}^3 \setminus \overline{\Omega_\delta}, \\ &[\![\boldsymbol{\nu} \times P\widetilde{\mathbf{a}}_L]\!] = \mathbf{0}, \\ &[\![\boldsymbol{\nu} \times \left(\mu^{-1}\nabla \times P\widetilde{\mathbf{a}}_L\right)]\!] = \mathrm{i}k\widetilde{\mathbf{a}}_L, \end{aligned}$$

and $P\widetilde{\mathbf{a}}_L$ is a radiating field. Therefore, $P\widetilde{\mathbf{a}}_L$ is the solution to (23), for $(\mathbf{h}_1, \mathbf{h}_2, \mathbf{h}_3)$ defined by (24), for $\mathbf{v} = -P\widetilde{\mathbf{a}}_L$, and $\mathscr{G}(\mathbf{h}_1, \mathbf{h}_2, \mathbf{h}_3) = \boldsymbol{\phi}^\infty_L$.

To prove the converse, let $\mathbf{a}_L \in \mathcal{C}^\infty_{0,t}(L)$ such that $\boldsymbol{\phi}^\infty_L \in Range(\mathscr{G})$. Then there is $(\mathbf{h}_1, \mathbf{h}_2, \mathbf{h}_3) \in \mathbf{H}(\mathrm{curl}_\Gamma, \Gamma_0) \times \mathcal{H}_0(\Gamma_0)^* \times \mathbf{H}^{-1/2}(\mathrm{div}_\mathscr{S}, \mathscr{S})$ such that $\mathbf{E}$ is a solution to (23) and its far field pattern satisfies $\mathbf{E}^\infty = \boldsymbol{\phi}^\infty_L$. On the other hand, $\boldsymbol{\phi}^\infty_L$ is also the far field pattern of the radiating field

$$\boldsymbol{\phi}_L(\mathbf{x}) := 4\pi \int_L \mathbb{G}^E(\mathbf{x}, \mathbf{y}_\gamma + \delta \mathbf{f}^+ \boldsymbol{\nu})\mathbf{a}_L(\mathbf{y}_\Gamma) \ \mathrm{d}\,\mathbf{y}_\Gamma.$$

By Rellich's lemma, $\mathbf{E}$ and $\boldsymbol{\phi}_L$ are identical in $\mathbb{R}^3 \setminus \overline{\Gamma_0 \cup L}$. Suppose $L \setminus \overline{\Gamma_0} \neq \emptyset$, then since $\mathbf{a}_L$ does not vanish in open sets of L there is $\mathbf{x} \in L \setminus \overline{\Gamma}_0$ such that $\mathbf{a}_L(\mathbf{x}) \neq 0$. Then $\boldsymbol{\nu} \times (\mu^{-1}\nabla \times \mathbf{E})$ would be continuous at $\mathbf{x}$ while $\boldsymbol{\nu} \times (\mu^{-1}\nabla \times \boldsymbol{\phi}_L)$ would have a jump at that same point, which is a contradiction. □

Proposition 3.2. *Under the same hypothesis of proposition 3.1, $\mathcal{F}_D : \mathbf{L}^2_t(\mathbb{S}^2) \to \mathbf{L}^2_t(\mathbb{S}^2)$ is injective with dense range.*

Proof. The fact that $\mathcal{F}_D = \mathscr{G}\mathscr{H}$ is injective is an immediate consequence of proposition 3.1 and from the injectivity of $\mathscr{G}$, which follows from the well-posedness of (23). To see that $\mathcal{F}_D$ has dense range, we consider $P : \mathbf{L}^2_t(\Gamma_0) \to \mathbf{L}^2_t(\mathbb{S}^2)$ defined by

$$(P\mathbf{a})(\widehat{\mathbf{d}}) = \frac{1}{4\pi} \int_{\Gamma_0} \mathbb{G}^{E,\infty}(\widehat{\mathbf{d}}, \mathbf{y})\mathbf{a}(\mathbf{y}) \ \mathrm{d}s(\mathbf{y}).$$

Then

$$\begin{aligned} (P\mathbf{a}, \mathbf{g})_{\mathbf{L}^2_t(\mathbb{S}^2)} &= 4\pi \int_{\mathbb{S}^2} \overline{\mathbf{g}(\widehat{\mathbf{d}})} \cdot \left\{ \int_{\Gamma_0} \mathbb{G}^{E,\infty}(\widehat{\mathbf{d}}, \mathbf{y})\mathbf{a}(\mathbf{y}) \ \mathrm{d}s(\mathbf{y}) \right\} \mathrm{d}s(\widehat{\mathbf{d}}) \\ &= \int_{\Gamma_0} \mathbf{a}(\mathbf{y}) \cdot \left\{ \int_{\mathbb{S}^2} \mathbf{E}_{pl}(\mathbf{y}, -\widehat{\mathbf{d}}, \overline{\mathbf{g}(\widehat{\mathbf{d}})}) \ \mathrm{d}s(\widehat{\mathbf{d}}) \right\} \mathrm{d}s(\mathbf{y}), \end{aligned}$$

thus

$$(P^*\mathbf{g})(\mathbf{y}) = \int_{\mathbb{S}^2} \overline{\mathbf{E}_{pl}(\mathbf{y}, -\widehat{\mathbf{d}}, \mathbf{g}(\widehat{\mathbf{d}}))}\ \mathrm{d}s(\widehat{\mathbf{d}}) = \overline{\mathbf{E}_{b,\widetilde{\mathbf{g}}}(\mathbf{y})},$$

where $\widetilde{\mathbf{g}} = \mathbf{g}(-\widehat{\mathbf{x}})$. Therefore, $P^*\mathbf{g} = \mathbf{0}$ if and only if $\mathbf{g} = \mathbf{0}$ and hence P has dense range. Since $Range(P) \subset Range(\mathcal{F}_D)$, the proof is complete. □

Now we are ready to prove the standard theorem that justifies the linear sampling method.

Theorem 3.3 (Linear sampling method). *Let $\mathcal{F}_D : \mathbf{L}_t^2(\mathbb{S}^2) \to \mathbf{L}_t^2(\mathbb{S}^2)$ be the far field operator given by (3.2). Then the following hold:*

1. *For any arbitrary open surface $L \subset \Gamma_0$ and $\varepsilon > 0$, there exists a $\mathbf{g}_\varepsilon \in \mathbf{L}_t^2(\mathbb{S}^2)$ such that*

$$\|\mathcal{F}_D\mathbf{g}_\varepsilon - \boldsymbol{\phi}_L^\infty\|_{\mathbf{L}_t^2(\mathbb{S}^2)} < \varepsilon,$$

   and, as $\varepsilon \to 0$, the corresponding solution $\mathbf{E}_{b,\mathbf{g}_\varepsilon}$ to the background problem (20) converges in $\mathcal{H}_0$ to the unique solution $\mathbf{E}_L$ of (23) where $\mathbf{h}_1$, $\mathbf{h}_2$ and $\mathbf{h}_3$ are given by (24), with $\mathbf{v} = \boldsymbol{\phi}_L^\infty$.
2. *For $L \not\subset \Gamma_0$ and $\varepsilon > 0$, every $\mathbf{g}_\varepsilon \in \mathbf{L}_t^2(\mathbb{S}^2)$ satisfying*

$$\|\mathcal{F}_D\mathbf{g}_\varepsilon - \boldsymbol{\phi}_L^\infty\|_{\mathbf{L}_t^2(\mathbb{S}^2)} \leqslant \varepsilon$$

   is such that the corresponding solution $\mathbf{E}_{b,\mathbf{g}_\varepsilon}$ to the background problem(20) satisfies

$$\lim_{\varepsilon\to 0} \|\mathbf{E}_{b,\mathbf{g}_\varepsilon}\|_{\mathbf{H}_{\mathrm{loc}}(\mathrm{curl},\mathbb{R}^3)} = \infty, \quad \text{and} \quad \lim_{\varepsilon\to 0} \|\mathbf{g}_\varepsilon\|_{\mathbf{L}_t^2(\mathbb{S}^2)} = \infty.$$

Remark 3.4. Theorem 3.3 is the basis of the nondestructive testing for the detection of the delaminated region $\Gamma_0 \subset \Gamma$. However, it is worth noticing that from the definition (25), the test functions correspond to far field patterns of potentials given by

$$\boldsymbol{\phi}_L(\mathbf{x}) := \int_L \mathbb{G}^E(\mathbf{x}, \mathbf{y}_\Gamma + \delta f^+ \boldsymbol{\nu})\mathbf{a}_L(\mathbf{y}_\Gamma)\ \mathrm{d}\,\mathbf{y}_\Gamma,$$

which are discontinuous on the shifted boundary

$$L_+ := \{\mathbf{y} = \mathbf{y}_\Gamma + \delta f^+ \boldsymbol{\nu}(\mathbf{y}_\gamma)d \,|\, \mathbf{y}_\gamma \in L\},$$

that in principle we do not know, since δf^+ is an unknown quantity. But if τ is a tangential vector to $L \subset \Gamma$ at $\mathbf{y}_\Gamma$, by the mixed reciprocity principle theorem 3.1,

$$4\pi\tau \cdot \mathbb{G}^{E,\infty}(\cdot, \mathbf{y}_\Gamma + \delta f^+ \boldsymbol{\nu}(\mathbf{y}_\Gamma))\mathbf{a}_L(\mathbf{y}_\Gamma) = \mathbf{a}_L(\mathbf{y}_\Gamma) \cdot \mathbf{E}_{pl}(\mathbf{y}_\Gamma + \delta f^+ \boldsymbol{\nu}(\mathbf{y}_\Gamma), -\cdot, \tau),$$

and since the tangential traces of $\mathbf{E}_{pl}(\cdot, -\widehat{\mathbf{x}}, \tau)$ are continuous, then if δ is small enough,

$$4\pi\tau \cdot \mathbb{G}^{E,\infty}(\cdot, \mathbf{y}_\Gamma + \delta f^+ \boldsymbol{\nu}(\mathbf{y}_\Gamma))\mathbf{a}_L(\mathbf{y}_\Gamma) \sim \mathbf{a}_L(\mathbf{y}_\Gamma) \cdot \mathbf{E}_{pl}(\mathbf{y}_\Gamma, -\cdot, \tau),$$

which can be computed because it is defined on the known surface Γ.

Remark 3.5. It is well-known that the linear sampling method is not fully justified since the criteria in theorem 3.3 is in terms of a norm depending on the unknown Γ_0 and furthermore

nothing can be said about the regularized solution to the far field equation. Other mathematically more rigorous methods, such as factorization method or the generalize linear sampling method, are adapted to inverse problems for surfaces (see e.g. [12, 27] and references therein). However, we cannot show that our complicated ATC's model for the delamination satisfies the assumptions needed for these methods to work.

4. Numerical experiments

In this section we develop a numerical algorithm for reconstructing the unknown delaminated part Γ_0 of the known interface Γ based on the linear sampling method stated in theorem 3.3, and present some preliminary numerical examples showing the viability of our reconstruction algorithm. Recall that our data is the electric far field pattern $\mathbf{E}^\infty(\widehat{\mathbf{x}}, \widehat{\mathbf{d}}, \mathbf{p})$ for $\widehat{\mathbf{x}}, \widehat{\mathbf{d}} \in \mathbb{S}_0^2 \subseteq \mathbb{S}^2$, where $\mathbb{S}_0^2$ is an open subset of the unit sphere, and three linearly independent polarization $\mathbf{p} \in \mathbb{R}^3$, and $\Omega_\pm$, $\epsilon_\pm$, $\mu_\pm$ and Γ are known but not ϵ_δ, μ_δ,f^+,f^-.

We use synthetic far field data computed using a finite element method for approximating the forward problem (8)–(12). This is implemented using the Netgen/NGSolve package [28], as described briefly in what follows (for more details see [11]).

For our numerical approximation of the Calderón map G_e, we use a spherical perfectly matched layer (PML) with outer radius R surrounding the obstacle (with an air layer between the PML and Ω). Therefore, instead of solving for the total field $\mathbf{E}$ everywhere, we solve for the scattered field $\mathbf{E}^s$ in $B_R \setminus \overline{\Omega}$ and for the total field $\mathbf{E}$ only in Ω.

The finite element solver is based on a variational formulation which is directly derived by multiplying the differential equations satisfied by $\mathbf{E}$ in Ω and $\mathbf{E}^s$ in Ω_{ext}, by a test function $\mathbf{v}$ that is allowed to be discontinuous across Γ_1 and integrating by parts in $B_R \setminus \overline{\Omega}$ and Ω. To handle the transmission conditions on Γ_1 between the exterior scattered field and interior total field, we use a standard Nitsche's formulation (an extension of the method in [23], see also [3]). Our numerical solver makes use of quadratic edge elements to discretize fields on volume domains and linear surface edge elements to discretize the ATCs when solving for $\mathcal{A}_1^{-1}$.

It is important to mention here that we do not use the ATC model to generate the forward data for the defective domain. Netgen/NGSolve allows meshing of a thin domain (using elements satisfying the maximum angle condition), so we can approximate the solution of the full Maxwell problem in both cases.

Two examples are used to illustrate the inversion scheme:

1. **The cube:** this example is for the configuration shown in the left panel of figure 3, were Ω_- is the interior of a cube, and the delamination is located on one side of the cube. The material geometrical parameters in this particular example are: $k = 3$, $\delta = 0.01$ and the outer boundary of the scatterer, Γ_1, is a sphere of radius $R_+ = 1.3$, and Γ is the surface of the cube centered at the origin and with side-length $l = 1.2$., whereas the physical material properties were chosen as $\mu_- = \mu_+ = \mu_\delta = 1$, $\epsilon_+ = 2 + 0.001i$, $\epsilon_- = 4 + 0.001i$, and $\epsilon_\delta = 3.5 + 0.001i$. In the numerical computations of the forward problem, we choose a spherical perfectly matched layer (PML) in the annular region $\{\mathbf{x} : 2 < |\mathbf{x}| < 2.7\}$, with absorption parameter $\alpha = 0.6$.
   Typical results for the forward solver are shown in the left column of figure 4. In this case the the direction of propagation of the incident plane wave is $\mathbf{d} = (1, 0, 0)$ and the polarization $\mathbf{p} = (0, 1, 0)$ (where the incident field is $\mathbf{E}^i(\mathbf{x}) = \mathbf{p}\exp(\mathrm{i}k\mathbf{d} \cdot \mathbf{x})$). Because the fields with and without the crack are quite close, we show only the scattered field with

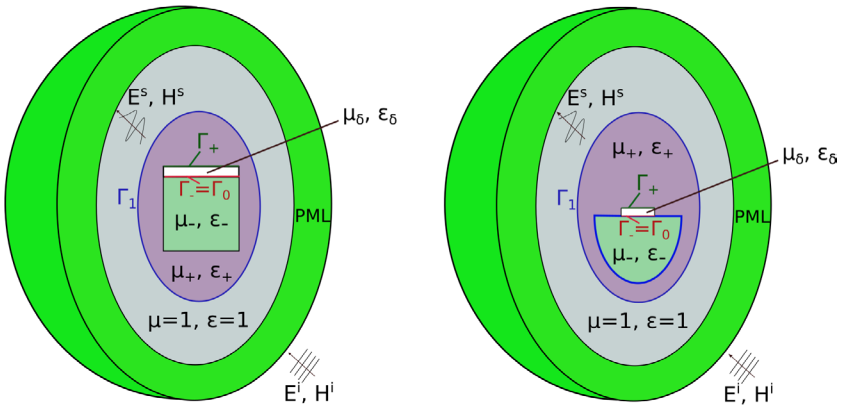

Figure 3. Schematics showing the setup of the numerical examples. In the left hand panel, showing the cube example, the delamination appears along the entire upper face of the cube. In the right hand panel, the delamination appears on a part of the planar face of the half-sphere.

the crack (middle row) and the difference between the field with and without the crack (lower row) of figure 4.

2. **The half-sphere:** for this second experiment, we consider a thin opening that does not cover completely the planar part of the interface Γ on the flat face of the half sphere (see figure 3 right panel). More specifically, we consider again a spherical obstacle Ω as shown in the right panel of figure 3, where the internal domain Ω_- is a half-sphere. The delamination Ω_δ has constant thickness and Γ_0 is a disk included on the flat part of Γ. As with the previous example, the radius of the exterior boundary Γ_1 is $R_+ = 1.3$, whereas the radius of the half-sphere that constitute the inner layer is $R_- = 0.6$. Moreover, the radius of the support of the delamination Γ_0 is 0.3 and it is centered at the origin. Again $\delta = 0.01$. We chose once again $\Gamma_- = \Gamma$, so that $f^- = 0$ and $f^+ = 1$.
   We consider two choices of material properties. Both are chosen to show that the method works for a dielectric scatterer.
   Change in shape: in the first example, the material properties are $\mu_+ = 1$, $\mu_- = 1.5$, $\mu_\delta = 1.5$, while $\epsilon_+ = 2$, $\epsilon_- = 3$ and $\epsilon_\delta = 3$. Notice that the properties of the 'delamination' are the same as for the inner material. In this case the delamination is actually a small change in the shape of the inner region Ω_-, and this problem is allowed by our theory. We make this choice to show that the method can detect small shape changes. Typical results for the forward solver are shown in the right hand column of figure 4.
   Delamination in a dielectric: for our final example we consider a model delamination problem for a dielectric. This material is assumed to be non-magnetic and the delamination is assumed to be filled with air. The material properties in this experiments are $\mu_+ = \mu_- = \mu_\delta = 1$, and $\epsilon_+ = 2$, $\epsilon_- = 3$, $\epsilon_\delta = 1$, and are chosen to show that the algorithm can work for a delamination in a dielectric. To save space we do not show forward data for this problem.

We next explain how the discretized far field operator and test functions are constructed. The procedure is based on [6], p 47. To this end let $\{\widehat{\mathbf{x}}_j\}_{j=1}^N \subset \mathbb{S}^2$ be the nodes and $\boldsymbol{\omega} = (\omega_1, ..., \omega_N)^T \in \mathbb{R}_+^N$ be the weights vector associated with a given quadrature rule on the

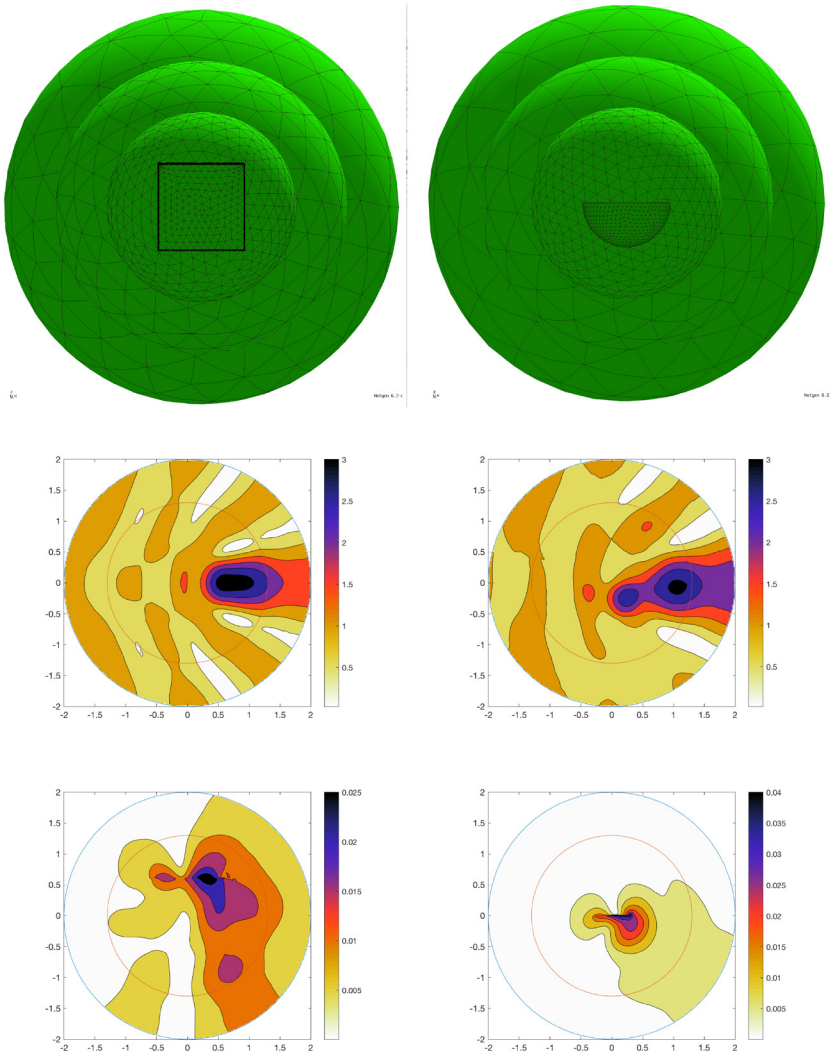

Figure 4. Forward data: the left hand column of the figure concerns the cube example (see left panel of figure 3), while the right hand is for the half sphere (see right panel of figure 3). All results are shown in the $x-z$ plane at $y=0$. The top row shows the surface meshes used including the PML. In these figures the crack is not easily visible on the upper face of the interior domain without magnification. The middle row shows the magnitude of the total field for the background configuration in the physical domain (i.e. not the PML). The bottom row shows the magnitude of the difference between the total field in the background and the flawed medium.

unit sphere $\mathbb{S}^2$. We will set both the incidence and the observation directions to coincide with $\{\widehat{\mathbf{x}}_j\}_{j=1}^N$. Therefore, the far-field operator acting on $\mathbf{g}\in\mathbf{L}_t^2(\mathbb{S}^2)^3$, satisfies

$$(\mathcal{F}\mathbf{g})(\widehat{\mathbf{x}}_i)=\int_{\mathbb{S}^2}\mathbf{E}^\infty(\widehat{\mathbf{x}}_i,\widehat{\mathbf{d}},\mathbf{g}(\widehat{\mathbf{d}}))\ \mathrm{d}s(\widehat{\mathbf{d}})\sim\sum_{j=1}^N\omega_j\mathbf{E}^\infty_{\mathrm{comp}}(\widehat{\mathbf{x}}_i,\widehat{\mathbf{x}}_j,\mathbf{g}(\widehat{\mathbf{x}}_j)).$$

Given $\widehat{\mathbf{x}}_j\times\mathbf{p}_j\neq 0$, if we define for every $j=1,...,N$, ,

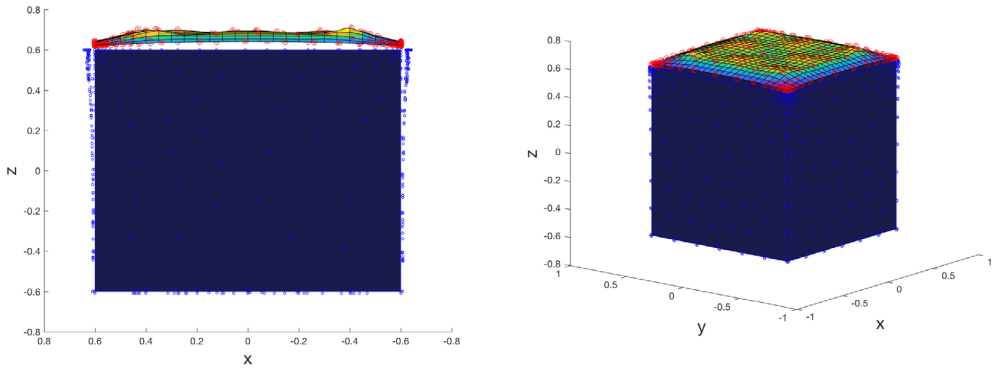

(a) (b)

Figure 5. Reconstruction of the delamination on the upper side of the cube, with $\varepsilon = 2 \times 10^{-5}$, and noise level $\rho \sim 0.059$.

$$\widehat{\mathbf{p}}_j^{\theta} := \frac{\mathbf{p}_j \times \widehat{\mathbf{x}}_j}{|\mathbf{p}_j \times \widehat{\mathbf{x}}_j|} \quad \text{and} \quad \widehat{\mathbf{p}}_j^{\phi} := \frac{\mathbf{p}_j \times (\widehat{\mathbf{x}}_j \times \mathbf{p}_j)}{|\mathbf{p}_j \times (\widehat{\mathbf{x}}_j \times \mathbf{p}_j)|},$$

and for $\ell \in \{\theta, \phi\}$ and $j \in \{1, ..., N\}$

$$g_j^{\ell} := \mathbf{g}(\widehat{\mathbf{x}}_j) \cdot \widehat{\mathbf{p}}_j^{\ell},$$

then by linearity,

$$\mathbf{E}^{\infty}_{\text{comp}}(\widehat{\mathbf{x}}_i, \widehat{\mathbf{x}}_j, \mathbf{g}(\widehat{\mathbf{x}}_j)) = \mathbf{E}^{\infty}_{\text{comp}}(\widehat{\mathbf{x}}_i, \widehat{\mathbf{x}}_j, \widehat{\mathbf{p}}_j^{\theta}) g_j^{\theta} + \mathbf{E}^{\infty}_{\text{comp}}(\widehat{\mathbf{x}}_i, \widehat{\mathbf{x}}_j, \widehat{\mathbf{p}}_j^{\phi}) g_j^{\phi}.$$

Thus denoting

$$\mathbf{A}_{i,j}^{\ell} = \mathbf{E}^{\infty}_{\text{comp}}(\widehat{\mathbf{x}}_i, \widehat{\mathbf{x}}_j, \widehat{\mathbf{p}}_j^{\ell}) \quad \text{for } \ell \in \{\theta, \phi\},$$

at the discrete level the associated far field equation becomes

$$\sum_{j=1}^{N} \omega_j \mathbf{A}_{i,j}^{\theta} g_j^{\theta} + \omega_j \mathbf{A}_{i,j}^{\phi} g_j^{\phi} = \boldsymbol{\phi}_{\mathbf{z}}^{\infty}(\widehat{\mathbf{x}}_i). \tag{26}$$

However, the discrete far-field equation (26) is in tensor form. To get a standard matrix equation we take the dot product of both sides of equation (26) with $\widehat{\mathbf{p}}_j^{\beta}$, for $\beta \in \{\theta, \phi\}$ and thus

$$\sum_{j=1}^{N} \omega_j \mathbf{A}_{i,j}^{\beta,\theta} g_j^{\theta} + \omega_j \mathbf{A}_{i,j}^{\beta,\phi} g_j^{\phi} = f_{\mathbf{z}}^{\beta}(\widehat{\mathbf{x}}_i),$$

where

$$\mathbf{A}_{i,j}^{\beta,\ell} := \widehat{\mathbf{p}}_i^{\beta} \cdot \mathbf{A}_{i,j}^{\ell} = \widehat{\mathbf{p}}_i^{\beta} \cdot \mathbf{E}^{\infty}_{\text{comp}}(\widehat{\mathbf{x}}_i, \widehat{\mathbf{x}}_j, \widehat{\mathbf{p}}_j^{\ell}) \quad \text{and} \quad f_{\mathbf{z}}^{\beta}(\widehat{\mathbf{x}}_i) := \widehat{\mathbf{p}}_i^{\beta} \cdot \boldsymbol{\phi}_{\mathbf{z}}^{\infty}(\widehat{\mathbf{x}}_i).$$

In matrix form, if $\mathbf{M}^{\ell,\beta} \in \mathbb{C}^{N \times N}$ is defined by

$$\mathbf{M}^{\ell,\beta} = \mathbf{A}^{\ell,\beta} \mathbf{D},$$

where $\mathbf{D} = \text{diag}\{\boldsymbol{\omega}\}$ is the diagonal matrix whose principal diagonal is the weights vector $\boldsymbol{\omega}$, then the far-field equation becomes

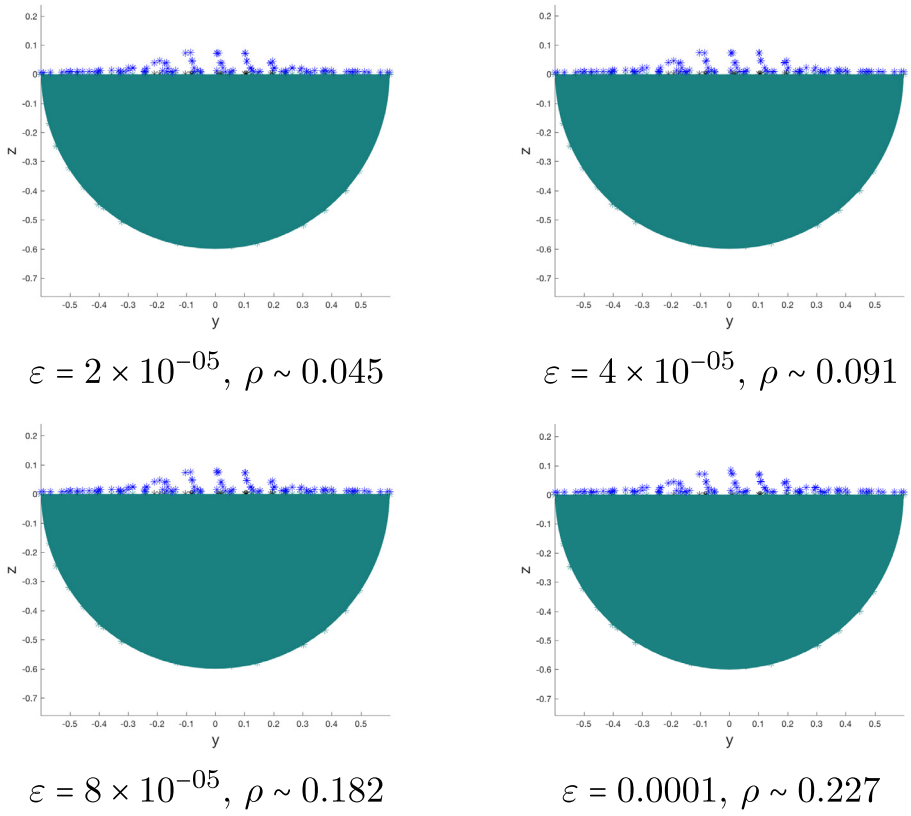

Figure 6. These results are for the shape change problem. We show a side view of the function $\chi_{\Gamma_+}(\mathbf{z})$, for the detection of a thin defect on a circular part of the flat boundary of the half sphere under different levels of noise ρ, and the corresponding values of ε. The separation of the blue dotted surface from the flat surface of the half sphere is proportional to the predicted location of the defect.

$$\left[\begin{array}{c|c} \mathbf{M}^{\theta,\theta} & \mathbf{M}^{\theta,\phi} \\ \hline \mathbf{M}^{\phi,\theta} & \mathbf{M}^{\phi,\phi} \end{array}\right]_{2N\times 2N} \left[\begin{array}{c} \mathbf{g}^{\theta} \\ \hline \mathbf{g}^{\phi} \end{array}\right]_{2N\times 1} = \left[\begin{array}{c} f_{\mathbf{z}}^{\theta} \\ \hline f_{\mathbf{z}}^{\phi} \end{array}\right]_{2N\times 1}.$$

As the discrete version of the ill-posed the far-field equation, this linear equation is also severely ill-posed and hence it is necessary to use regularization techniques, for example, the standard Tikhonov regularization method. Given the solution $\mathbf{g}_{\mathbf{z},\eta}$ to the regularized problem associated to the regularization parameter $0 < \eta$, the indicator function that we compute is given by

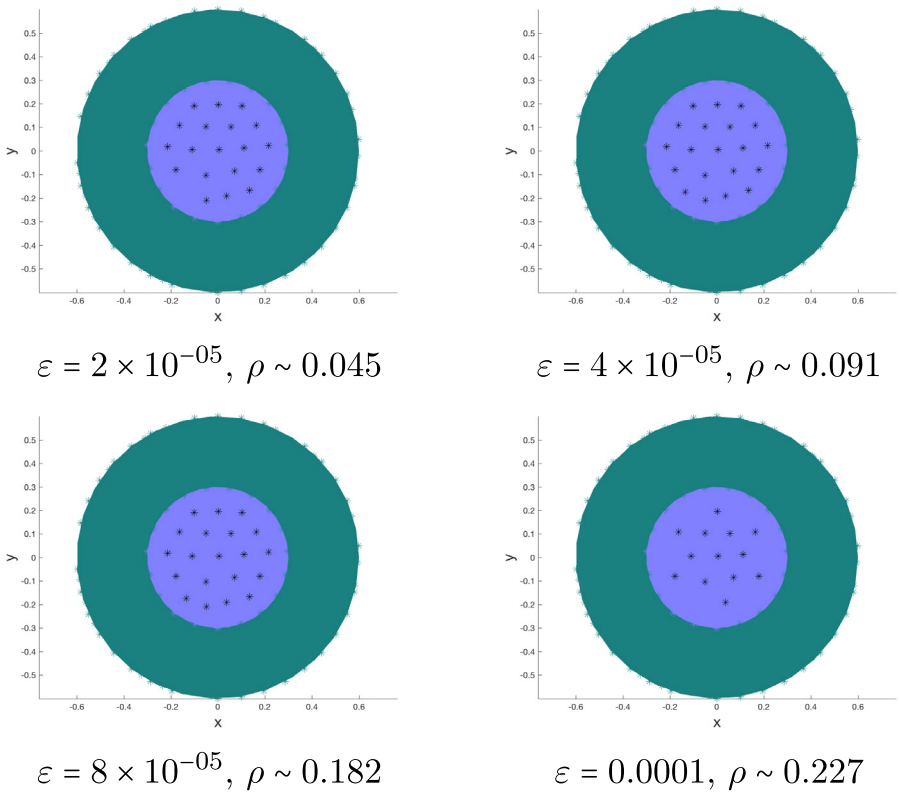

Figure 7. These results are for the shape change problem. We show reconstructions of shape change due to a thin defect on a circular part of the flat boundary of the half sphere Ω_- under different levels of noise ρ, and the corresponding values of ε. The blue circle is the exact location of the defect and the black dots correspond to the predicted location of the defect, i.e. the support of the truncated function G_η, when the threshold values is $\tau = 0.5 * \max\{G_\eta(\mathbf{z}) \,|\, \mathbf{z} \in \Gamma_0\}$.

$$G_\eta(\mathbf{z}) = 1/||\mathbf{g}_{\mathbf{z},\eta}||.$$

In our case, for the practical examples, the test function will be considered when the surface $L \subset \Gamma$ shrinks to the point $\mathbf{z}$ and the density $\mathbf{a}_L$ tends to a delta function $\delta(\cdot - \mathbf{z})\boldsymbol{\tau}_\ell$, where $\boldsymbol{\tau}_\ell$ for $\ell = 1, 2$ are the basis of the tangential plane to Γ at $\mathbf{z}$. In such a case,

$$\boldsymbol{\phi}^\infty_{\mathbf{z},\ell}(\widehat{\mathbf{x}}_i) = \mathbb{G}^{E,\infty}(\widehat{\mathbf{x}}_i, \mathbf{z} + \delta f^+ \boldsymbol{\nu})\boldsymbol{\tau}_\ell \quad \text{for} \quad \ell = 1, 2.$$

Then the terms in the right-hand-side for the discrete far field equation are

$$\begin{aligned} f^\beta_{\mathbf{z},\ell}(\widehat{\mathbf{x}}_i) &= \widehat{\mathbf{p}}^\beta_i \cdot \boldsymbol{\phi}^\infty_{\mathbf{z},\ell}(\widehat{\mathbf{x}}_i) = \widehat{\mathbf{p}}^\beta_i \cdot \mathbb{G}^{E,\infty}(\widehat{\mathbf{x}}_i, \mathbf{z} + \delta f^+ \boldsymbol{\nu})\boldsymbol{\tau}_\ell \\ &= \frac{1}{4\pi}\boldsymbol{\tau}_\ell \cdot \mathbf{E}_b(\mathbf{z} + \delta f^+ \boldsymbol{\nu}, -\widehat{\mathbf{x}}_i, \widehat{\mathbf{p}}^\beta_i) \sim \frac{1}{4\pi}\boldsymbol{\tau}_\ell \cdot \mathbf{E}_b(\mathbf{z}, -\widehat{\mathbf{x}}_i, \widehat{\mathbf{p}}^\beta_i). \end{aligned} \tag{27}$$

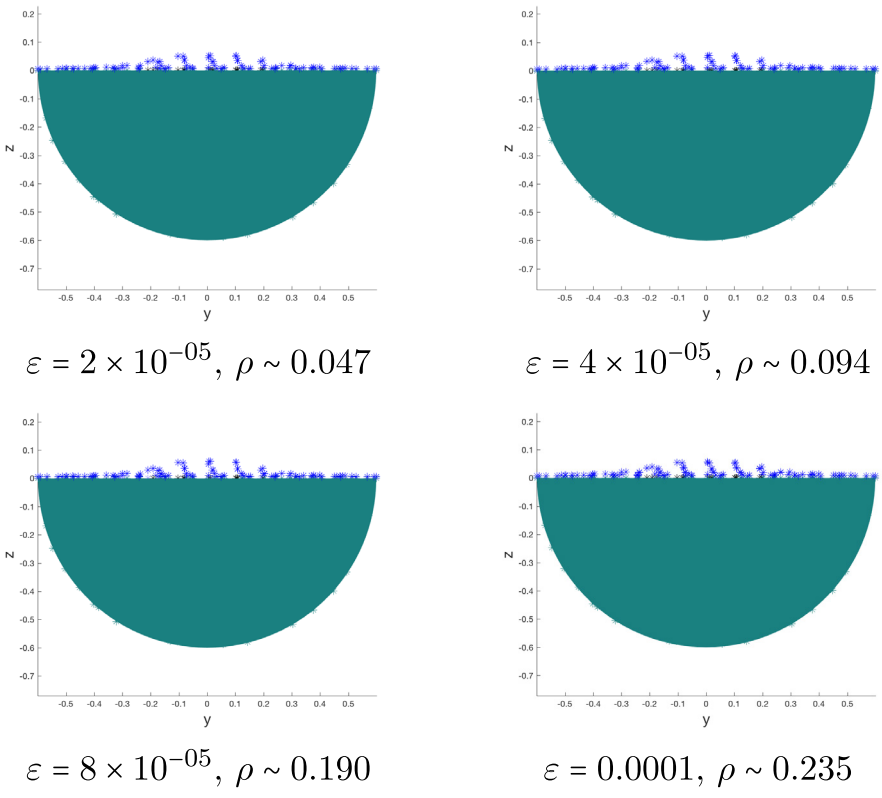

Figure 8. These results are for the dielectric delaimination problem. We show a side view of the function $\chi_{\Gamma_+}(\mathbf{z})$, for the detection of a delamination on a circular part of the flat boundary of the half sphere under different levels of noise ρ, and the corresponding values of ε. The separation of the blue dotted surface from the flat surface of the half sphere is proportional to the predicted location of the delamination.

4.1. Example 1: the cube

We first consider the cube in which the top face is entirely delaminated. Data is generated as described earlier in this section. In total, the number of incident directions $\widehat{\mathbf{d}} \in \mathbb{S}^2$ is 93, and they are generated as the nodes of an approximately uniform surface mesh on the unit sphere $\mathbb{S}^2$ constructed by Netgen/Ngsolve [28]. The sampling points $\{\mathbf{z}_\ell\}_{\ell=1}^{N_s}$, $N_s = 152$, are constructed in a similar way, by defining a surface mesh on the cube.

The regularization parameter for the Tikhonov regularization method in this example is chosen $\eta = 10^{-10}$.

Both the far field data and the right-hand-side (27) are computed by solving the full problem (1) - (2) using a finite element method as in [11]. The mesh refinement level is set to be $h_{max} = 0.2$. Some noise in the data is added in order to avoid inverse crimes.

We consider $\tilde{A}_{ij} = A_{ij}(1 + \varepsilon\zeta_{ij})$, where $\{\zeta_{ij}\}$ is a collection of independent random variables with uniform distribution over the interval $[-1, 1]$, and $\varepsilon > 0$ is a constant. The level of noise is defined by $\rho := ||A - \tilde{A}||_2/||A||_2$.

For visualization purposes, in our reconstruction in figure 5, the separation of the dotted surfaces $\tilde{\Gamma}_\pm$ is chosen to be proportional to $G_\eta(\mathbf{z})$, with the parametrization

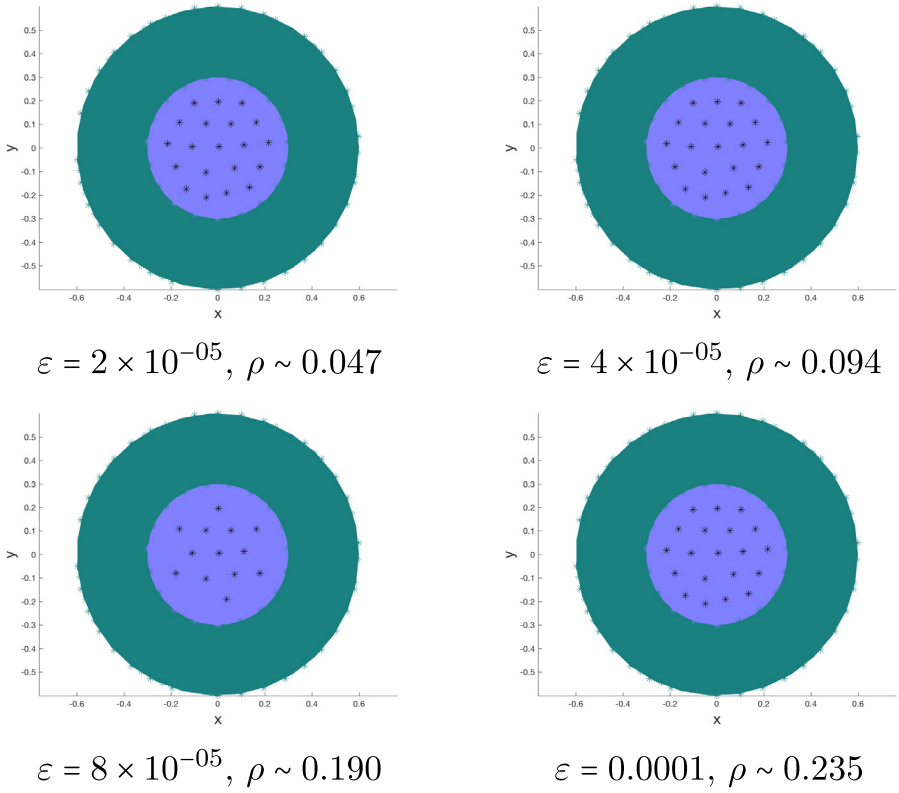

Figure 9. These examples are for the dielectric delamination problem. We show reconstructions of the delamination on a circular part of the flat boundary of the half sphere under different levels of noise ρ, and the corresponding values of ε. The blue circle is the exact location of the delamination and the black dots correspond to the predicted location of the delamination, i.e. the support of the truncated function G_η, when the threshold values is $\tau = 0.5 * \max\{G_\eta(\mathbf{z}) \,|\, \mathbf{z} \in \Gamma_0\}$.

$$\chi_{\tilde{\Gamma}_+}(t) = \chi_\Gamma(t) + \eta_0 G_\eta(\chi_\Gamma(t))\boldsymbol{\nu}(t),$$

where χ_Γ is the parametrization of Γ, and we arbitrarily set $\eta_0 = 70$ as a constant that modulates the size of G_η for pure visualization purposes. The separation of the dotted surfaces $\tilde{\Gamma}_+$ from the reference surface Γ corresponds, therefore, to the areas where our algorithm predicts the location of the delamination, but not the thickness

4.2. Example 2: half-sphere

The same number and directions of the incident fields as for the previous example are used in this case. We now consider the two experiments outlined earlier in this section:

4.3. Change in shape

Results for the reconstruction of the change in shape due to a a thin defect on the boundary are shown in figures 6 and 7. In figure 6, we use the same visualization procedure

as in the previous example, although in this case we analyze the quality of the reconstruction with respect to four different noise levels ρ, and the corresponding amplitude parameter of the uniform random noise ε. In figure 9, the reconstruction of the delaminated part of Γ is shown for the same levels of noise when the truncation value of G_η is $\tau = 0.5 * \max\{G_\eta(\mathbf{z}) \,|\, \mathbf{z} \in \Gamma_0\}$.

4.4. Delamiation in a dielectric

For this example in which the delamination is an air-filled region between two dissimilar dielectric regions, the the reconstructions are shown in figures 8 and 9. The visualization is carried out in the same way as for the previous example. The crack is clearly detected.

5. Conclusion

A linear sampling method algorithm based on a Chun's-type ATCs model is developed that efficiently tests for delamination on flat interfaces between two materials. Numerical examples indicate that our reconstruction method provides qualitatively good results also with noisy data and is stable with respect to a reasonable noise level. However it is well-known that all linear sampling methods suffer from instability with respect to errors in the modeling of the background. Efforts have been made to address this issue [4], but we will not address it any further since it is beyond the scope of our study.

Our analysis requires that the delamination is a volume with constant thickness. Of course this situation is far from many realistic cases of non-destructive testing of interfaces. Unfortunately, the analysis of the ATCs model that includes a curved opening with variable thickness is still an open problem (see [11] for the explicit reasons) and therefore there is no analytical framework to develop the inversion scheme. Nevertheless, we expect that a formal application of the linear sampling method, i.e. an implementation of the equation (26), could yield reasonable reconstructions in more realistic general cases. Unfortunately, the lack of a well-posed variational formulation for the general case, prevents us from computing the data in order to test the latter claim.

Acknowledgments

The research of F Cakoni is supported in part by AFOSR Grant FA9550-17-1-0147, NSF Grant DMS-1602802 and Simons Foundation Award 392261. The research of P Monk is supported in part by AFOSR Grant FA9550-17-1-0147. This work is derived in part from the PhD thesis of I de Teresa [11].

Appendix A. Proof of theorem 3.1

Proof. First for simplicity of presentation here we drop the subindex 'b' in the notation of the background electric and magnetic field. We need to consider several cases.

Case 1 . We first assume that $\mathbf{z} \in \mathbb{R}^3 \setminus \overline{\Omega}$. Let $\mathbf{p}, \mathbf{q} \in \mathbb{R}^3$. Since in this case the pair

$$(\mathbf{E}, \mathbf{H}) = \left(\mathbb{G}^E(\cdot, \mathbf{z})\mathbf{q} - \mathbf{E}^i_{edp}(\cdot, \mathbf{z}, \mathbf{q}),\ \mathbb{G}^H(\cdot, \mathbf{z})\mathbf{q} - \mathbf{H}^i_{edp}(\cdot, \mathbf{z}, \mathbf{q})\right)$$

is a radiating and non-singular solution of the homogeneous Maxwell equations (19) in $\mathbb{R}^3 \setminus \overline{\Omega}$, we can use the Stratton–Chu formula for radiating fields (see [21], theorem 9.4):

$$\mathbb{G}^E(\mathbf{x},\mathbf{z})\mathbf{q} - \mathbf{E}^i_{edp}(\mathbf{x},\mathbf{z},\mathbf{q}) = \nabla_x \times \int_{\Gamma_1} \boldsymbol{\nu}(\mathbf{y}) \times (\mathbb{G}^E(\mathbf{y},\mathbf{z})\mathbf{q} - \mathbf{E}^i_{edp}(\mathbf{y},\mathbf{z},\mathbf{q}))\phi(\mathbf{x},\mathbf{y})\ \mathrm{d}s(\mathbf{y}) - \frac{1}{\mathrm{i}k}\nabla_x \times \nabla_x \times \int_{\Gamma_1} \boldsymbol{\nu}(\mathbf{y}) \times (\mathbb{G}^H(\mathbf{y},\mathbf{z})\mathbf{q} - \mathbf{H}^i_{edp}(\mathbf{y},\mathbf{z},\mathbf{q}))\phi(\mathbf{x},\mathbf{y})\ \mathrm{d}s(\mathbf{y}), \tag{A.1}$$

for all $\mathbf{x} \in \mathbb{R}^3 \setminus \overline{\Omega}$. On the other hand, for any constant $\mathbf{p} \in \mathbb{R}^3$, taking the dot product of $\mathbf{p}$ with the terms in the right-hand-side of the Stratton–Chu formula (A.1) involving the electric dipole fields $\mathbf{E}^i_{edp}$ and $\mathbf{H}^i_{edp}$, we obtain

$$\begin{aligned}
&\mathbf{p}\cdot\nabla_x \times \int_{\Gamma_1} (\boldsymbol{\nu}(\mathbf{y}) \times \mathbf{E}^i_{edp}(\mathbf{y},\mathbf{z},\mathbf{q}))\phi(\mathbf{x},\mathbf{y})\ \mathrm{d}s(\mathbf{y}) \\
&\quad - \frac{1}{\mathrm{i}k}\mathbf{p}\cdot\nabla_x \times \nabla_x \times \int_{\Gamma_1} (\boldsymbol{\nu}(\mathbf{y}) \times \mathbf{H}^i_{edp}(\mathbf{y},\mathbf{z},\mathbf{q}))\phi(\mathbf{x},\mathbf{y})\ \mathrm{d}s(\mathbf{y}) \\
&= -\int_{\Gamma_1} (\boldsymbol{\nu}(\mathbf{y}) \times \mathbf{E}^i_{edp}(\mathbf{y},\mathbf{z},\mathbf{q}))\cdot\nabla_y \times (\mathbf{p}\phi(\mathbf{x},\mathbf{y}))\ \mathrm{d}s(\mathbf{y}) \\
&\quad - \frac{1}{\mathrm{i}k}\int_{\Gamma_1} (\boldsymbol{\nu}(\mathbf{y}) \times \mathbf{H}^i_{edp}(\mathbf{y},\mathbf{z},\mathbf{q}))\cdot\nabla_y \times \nabla_y \times (\mathbf{p}\phi(\mathbf{x},\mathbf{y}))\ \mathrm{d}s(\mathbf{y}) \\
&= \int_{\Gamma_1} (\boldsymbol{\nu}(\mathbf{y}) \times \mathbf{E}^i_{edp}(\mathbf{y},\mathbf{z},\mathbf{q}))\cdot\mathbf{H}^i_{edp}(\mathbf{x},\mathbf{y},\mathbf{p})\ \mathrm{d}s(\mathbf{y}) \\
&\quad + \int_{\Gamma_1} (\boldsymbol{\nu}(\mathbf{y}) \times \mathbf{H}^i_{edp}(\mathbf{y},\mathbf{z},\mathbf{q}))\cdot\mathbf{E}^i_{edp}(\mathbf{x},\mathbf{y},\mathbf{p})\ \mathrm{d}s(\mathbf{y}),
\end{aligned}$$

thus,

$$\begin{aligned}
&\mathbf{p}\cdot\nabla_x \times \int_{\Gamma_1} (\boldsymbol{\nu}(\mathbf{y}) \times \mathbf{E}^i_{edp}(\mathbf{y},\mathbf{z},\mathbf{q}))\phi(\mathbf{x},\mathbf{y})\ \mathrm{d}s(\mathbf{y}) \\
&\quad - \frac{1}{\mathrm{i}k}\mathbf{p}\cdot\nabla_x \times \nabla_x \times \int_{\Gamma_1} (\boldsymbol{\nu}(\mathbf{y}) \times \mathbf{H}^i_{edp}(\mathbf{y},\mathbf{z},\mathbf{q}))\phi(\mathbf{x},\mathbf{y})\ \mathrm{d}s(\mathbf{y}) \\
&= -\int_{\Gamma_1} (\boldsymbol{\nu}(\mathbf{y}) \times \mathbf{E}^i_{edp}(\mathbf{y},\mathbf{z},\mathbf{q}))\cdot\nabla_y \times (\mathbf{p}\phi(\mathbf{x},\mathbf{y}))\ \mathrm{d}s(\mathbf{y}) \\
&\quad - \frac{1}{\mathrm{i}k}\int_{\Gamma_1} (\boldsymbol{\nu}(\mathbf{y}) \times \mathbf{H}^i_{edp}(\mathbf{y},\mathbf{z},\mathbf{q}))\cdot\nabla_y \times \nabla_y \times (\mathbf{p}\phi(\mathbf{x},\mathbf{y}))\ \mathrm{d}s(\mathbf{y}) \\
&= \int_\Omega \{\nabla \times \mathbf{E}^i_{edp}(\mathbf{y},\mathbf{z},\mathbf{q}))\cdot\mathbf{H}^i_{edp}(\mathbf{x},\mathbf{y},\mathbf{p})\}\ \mathrm{d}\mathbf{y} - \int_\Omega \{(\nabla \times \mathbf{H}^i_{edp}(\mathbf{x},\mathbf{y},\mathbf{p}))\cdot\mathbf{E}^i_{edp}(\mathbf{y},\mathbf{z},\mathbf{q})\}\ \mathrm{d}\mathbf{y} \\
&\quad + \int_\Omega \{\nabla \times \mathbf{H}^i_{edp}(\mathbf{y},\mathbf{z},\mathbf{q}))\cdot\mathbf{E}^i_{edp}(\mathbf{x},\mathbf{y},\mathbf{p})\}\ \mathrm{d}\mathbf{y} - \int_\Omega \{(\nabla \times \mathbf{E}^i_{edp}(\mathbf{x},\mathbf{y},\mathbf{p}))\cdot\mathbf{H}^i_{edp}(\mathbf{y},\mathbf{z},\mathbf{q})\}\ \mathrm{d}\mathbf{y},
\end{aligned}$$

and therefore,

$$\begin{aligned}
&\mathbf{p}\cdot\nabla_x \times \int_{\Gamma_1} (\boldsymbol{\nu}(\mathbf{y}) \times \mathbf{E}^i_{edp}(\mathbf{y},\mathbf{z},\mathbf{q}))\phi(\mathbf{x},\mathbf{y})\ \mathrm{d}s(\mathbf{y}) \\
&\quad - \frac{1}{\mathrm{i}k}\mathbf{p}\cdot\nabla_x \times \nabla_x \times \int_{\Gamma_1} (\boldsymbol{\nu}(\mathbf{y}) \times \mathbf{H}^i_{edp}(\mathbf{y},\mathbf{z},\mathbf{q}))\phi(\mathbf{x},\mathbf{y})\ \mathrm{d}s(\mathbf{y}) \\
&= -\int_{\Gamma_1} (\boldsymbol{\nu}(\mathbf{y}) \times \mathbf{E}^i_{edp}(\mathbf{y},\mathbf{z},\mathbf{q}))\cdot\nabla_y \times (\mathbf{p}\phi(\mathbf{x},\mathbf{y}))\ \mathrm{d}s(\mathbf{y}) \\
&\quad - \frac{1}{\mathrm{i}k}\int_{\Gamma_1} (\boldsymbol{\nu}(\mathbf{y}) \times \mathbf{H}^i_{edp}(\mathbf{y},\mathbf{z},\mathbf{q}))\cdot\nabla_y \times \nabla_y \times (\mathbf{p}\phi(\mathbf{x},\mathbf{y}))\ \mathrm{d}s(\mathbf{y}).
\end{aligned}$$

Hence we further obtain

$$\begin{aligned}
&\mathbf{p}\cdot\nabla_x\times\int_{\Gamma_1}(\boldsymbol{\nu}(\mathbf{y})\times\mathbf{E}^i_{edp}(\mathbf{y},\mathbf{z},\mathbf{q}))\phi(\mathbf{x},\mathbf{y})\ \mathrm{d}s(\mathbf{y})\\
&=\int_\Omega\{\mathrm{i}k\mathbf{H}^i_{edp}(\mathbf{y},\mathbf{z},\mathbf{q})\cdot\mathbf{H}^i_{edp}(\mathbf{x},\mathbf{y},\mathbf{p})\}\ \mathrm{d}\,\mathbf{y}+\int_\Omega\{\mathrm{i}k\mathbf{E}^i_{edp}(\mathbf{x},\mathbf{y},\mathbf{p})\cdot\mathbf{E}^i_{edp}(\mathbf{y},\mathbf{z},\mathbf{q})\}\ \mathrm{d}\,\mathbf{y}\\
&\quad+\int_\Omega\{-\mathrm{i}k\mathbf{E}^i_{edp}(\mathbf{y},\mathbf{z},\mathbf{q})\cdot\mathbf{E}^i_{edp}(\mathbf{x},\mathbf{y},\mathbf{p})\}\ \mathrm{d}\,\mathbf{y}-\int_\Omega\{\mathrm{i}k\mathbf{H}^i_{edp}(\mathbf{x},\mathbf{y},\mathbf{p})\cdot\mathbf{H}^i_{edp}(\mathbf{y},\mathbf{z},\mathbf{q})\}\ \mathrm{d}\,\mathbf{y}=0,
\end{aligned}$$

which implies that (A.1) simplifies to

$$\begin{aligned}
\mathbb{G}^E(\mathbf{x},\mathbf{z})\mathbf{q}-\mathbf{E}^i_{edp}(\mathbf{x},\mathbf{z},\mathbf{q})&=\nabla_x\times\int_{\Gamma_1}(\boldsymbol{\nu}(\mathbf{y})\times\mathbb{G}^E(\mathbf{y},\mathbf{z})\mathbf{q})\phi(\mathbf{x},\mathbf{y})\ \mathrm{d}s(\mathbf{y})\\
&\quad-\frac{1}{\mathrm{i}k}\nabla_x\times\nabla_x\times\int_{\Gamma_1}(\boldsymbol{\nu}(\mathbf{y})\times\mathbb{G}^H(\mathbf{y},\mathbf{z})\mathbf{q})\phi(\mathbf{x},\mathbf{y})\ \mathrm{d}s(\mathbf{y}),
\end{aligned}\tag{A.2}$$

for all $\mathbf{x}\in\mathbb{R}^3\setminus\overline{\Omega}$. Therefore, by taking the dot product of a constant vector $\mathbf{p}\in\mathbb{R}^3$ with (A.2), we know that the far field patterns satisfy

$$\begin{aligned}
&\mathbf{p}\cdot(\mathbb{G}^{E,\infty}(\widehat{\mathbf{x}},\mathbf{z})\mathbf{q})-\mathbf{p}\cdot\mathbf{E}^{i,\infty}_{edp}(\widehat{\mathbf{x}},\mathbf{z},\mathbf{q})\\
&=\frac{\mathrm{i}k}{2\pi}\mathbf{p}\cdot\{\widehat{\mathbf{x}}\times\int_{\Gamma_1}\{(\boldsymbol{\nu}(\mathbf{y})\times\mathbb{G}^E(\mathbf{y},\mathbf{z})\mathbf{q})+(\boldsymbol{\nu}(\mathbf{y})\times\mathbb{G}^H(\mathbf{y},\mathbf{z})\mathbf{q})\times\widehat{\mathbf{x}}\}\mathrm{e}^{-\mathrm{i}k\widehat{\mathbf{x}}\cdot\mathbf{y}}\ \mathrm{d}s(\mathbf{y})\}\\
&=\frac{\mathrm{i}k}{2\pi}\int_{\Gamma_1}(\boldsymbol{\nu}(\mathbf{y})\times\mathbb{G}^E(\mathbf{y},\mathbf{z})\mathbf{q})\cdot(-\widehat{\mathbf{x}}\times\mathbf{p})\mathrm{e}^{-\mathrm{i}k\widehat{\mathbf{x}}\cdot\mathbf{y}}\\
&\quad+(\boldsymbol{\nu}(\mathbf{y})\times\mathbb{G}^H(\mathbf{y},\mathbf{z})\mathbf{q})\cdot((-\widehat{\mathbf{x}})\times(\mathbf{p}\times(-\widehat{\mathbf{x}}))\mathrm{e}^{-\mathrm{i}k\widehat{\mathbf{x}}\cdot\mathbf{y}}\ \mathrm{d}s(\mathbf{y})\\
&=\frac{1}{2\pi}\int_{\Gamma_1}(\boldsymbol{\nu}(\mathbf{y})\times\mathbb{G}^E(\mathbf{y},\mathbf{z})\mathbf{q})\cdot\mathbf{H}^i_{pl}(\mathbf{y},-\widehat{\mathbf{x}},\mathbf{p})+(\boldsymbol{\nu}(\mathbf{y})\times\mathbb{G}^H(\mathbf{y},\mathbf{z})\mathbf{q})\cdot\mathbf{E}^i_{pl}(\mathbf{y},-\widehat{\mathbf{x}},\mathbf{p})\ \mathrm{d}s(\mathbf{y}),
\end{aligned}\tag{A.3}$$

for all $\widehat{\mathbf{x}}\in\mathbb{S}^2$. On the other hand,

$$\begin{aligned}
\mathbf{p}\cdot\mathbf{E}^{i,\infty}_{edp}(\widehat{\mathbf{x}},\mathbf{z},\mathbf{q})&=-\frac{1}{i4\pi k}\mathbf{p}\cdot\nabla_z\times\nabla_z\times(\mathbf{q}\mathrm{e}^{-\mathrm{i}k\widehat{\mathbf{x}}\cdot z})=\frac{\mathrm{i}k}{4\pi}\mathbf{p}\cdot(-\widehat{\mathbf{x}}\times(-\widehat{\mathbf{x}}\times\mathbf{q}))\mathrm{e}^{-\mathrm{i}k\widehat{\mathbf{x}}\cdot z}\\
&=\frac{\mathrm{i}k}{4\pi}\mathbf{q}\cdot((-\widehat{\mathbf{x}}\times\mathbf{p})\times(-\widehat{\mathbf{x}}))\mathrm{e}^{-\mathrm{i}k\widehat{\mathbf{x}}\cdot z}=\frac{1}{4\pi}\mathbf{q}\cdot\mathbf{E}^i_{pl}(\mathbf{z},-\widehat{\mathbf{x}},\mathbf{p}),
\end{aligned}$$

and

$$\begin{aligned}
\mathbf{p}\cdot\mathbf{H}^{i,\infty}_{edp}(\widehat{\mathbf{x}},\mathbf{z},\mathbf{q})&=-\frac{1}{4\pi}\mathbf{p}\cdot\nabla_z\times(\mathbf{q}\mathrm{e}^{-\mathrm{i}k\widehat{\mathbf{x}}\cdot z})=-\frac{\mathrm{i}k}{4\pi}\mathbf{p}\cdot(-\widehat{\mathbf{x}}\times\mathbf{q})\mathrm{e}^{-\mathrm{i}k\widehat{\mathbf{x}}\cdot z}\\
&=\frac{\mathrm{i}k}{4\pi}\mathbf{q}\cdot(-\widehat{\mathbf{x}}\times\mathbf{p})\mathrm{e}^{-\mathrm{i}k\widehat{\mathbf{x}}\cdot z}=\frac{1}{4\pi}\mathbf{q}\cdot\mathbf{H}^i_{pl}(\mathbf{z},-\widehat{\mathbf{x}},\mathbf{p}).
\end{aligned}$$

Hence, (A.3) can be written as

$$\begin{aligned}
&\mathbf{p}\cdot(\mathbb{G}^{E,\infty}(\widehat{\mathbf{x}},\mathbf{z})\mathbf{q})-\frac{\mathrm{i}k}{4\pi}\mathbf{q}\cdot\mathbf{E}^i_{pl}(\mathbf{z},-\widehat{\mathbf{x}},\mathbf{p})\\
&=\frac{1}{4\pi}\int_{\Gamma_1}(\boldsymbol{\nu}(\mathbf{y})\times\mathbb{G}^E(\mathbf{y},\mathbf{z})\mathbf{q})\cdot\mathbf{H}^i_{pl}(\mathbf{y},-\widehat{\mathbf{x}},\mathbf{p})\ \mathrm{d}s(\mathbf{y})\\
&\quad+\frac{1}{4\pi}\int_{\Gamma_1}(\boldsymbol{\nu}(\mathbf{y})\times\mathbb{G}^H(\mathbf{y},\mathbf{z})\mathbf{q})\cdot\mathbf{E}^i_{pl}(\mathbf{y},-\widehat{\mathbf{x}},\mathbf{p})\ \mathrm{d}s(\mathbf{y}),
\end{aligned}\tag{A.4}$$

for all $\widehat{\mathbf{x}} \in \mathbb{S}^2$. We will now show that the right hand side of (A.4) is exactly $\frac{1}{4\pi}\mathbf{q} \cdot \mathbf{E}^s_{pl}(\mathbf{z}, -\widehat{\mathbf{x}}, \mathbf{p})$.

To this end, observe that on one hand, by Green's formula, for any two given solutions $(\mathbf{E}_1, \mathbf{H}_1)$ and $(\mathbf{E}_2, \mathbf{H}_2)$ to the homogeneous Maxwell's equations (19) in Ω we have

$$\begin{aligned}
&\int_{\Gamma_1} (\boldsymbol{\nu}(\mathbf{y}) \times \mathbf{E}_1(\mathbf{y})) \cdot \mathbf{H}_2(\mathbf{y}) \ \mathrm{d}s(\mathbf{y}) + \int_{\Gamma_1} (\boldsymbol{\nu}(\mathbf{y}) \times \mathbf{H}_1(\mathbf{y})) \cdot \mathbf{E}_2(\mathbf{y}) \ \mathrm{d}s(\mathbf{y}) \\
&= \int_{\Omega} \{\nabla_y \times \mathbf{E}_1(\mathbf{y}) \cdot \mathbf{H}_2(\mathbf{y}) - \nabla_y \times \mathbf{H}_2(\mathbf{y}) \cdot \mathbf{E}_1(\mathbf{y})\} \ \mathrm{d}\mathbf{y} \\
&+ \int_{\Omega} \{\nabla_y \times \mathbf{H}_1(\mathbf{y}) \cdot \mathbf{E}_2(\mathbf{y}) - \nabla_y \times \mathbf{E}_2(\mathbf{y}) \cdot \mathbf{H}_1(\mathbf{y})\} \ \mathrm{d}\mathbf{y} = \mathbf{0},
\end{aligned} \tag{A.5}$$

while on the other hand, if both $(\mathbf{E}_1, \mathbf{H}_1)$ and $(\mathbf{E}_2, \mathbf{H}_2)$ satisfy the background problem (20) in Ω,

$$\begin{aligned}
&\int_{\Gamma_1} \boldsymbol{\nu}(\mathbf{y}) \times \mathbf{E}_1(\mathbf{y}) \cdot \mathbf{H}_2(\mathbf{y}) \ \mathrm{d}s(\mathbf{y}) + \int_{\Gamma_1} \boldsymbol{\nu}(\mathbf{y}) \times \mathbf{H}_1(\mathbf{y}) \cdot \mathbf{E}_2(\mathbf{y}) \ \mathrm{d}s(\mathbf{y}) \\
&= \int_{\Omega} \{\nabla_y \times \mathbf{E}_1(\mathbf{y}) \cdot \mathbf{H}_2(\mathbf{y}) - \nabla_y \times \mathbf{H}_2(\mathbf{y}) \cdot \mathbf{E}_1(\mathbf{y})\} \ \mathrm{d}\mathbf{y} \\
&+ \int_{\Omega} \{\nabla_y \times \mathbf{H}_1(\mathbf{y}) \cdot \mathbf{E}_2(\mathbf{y}) - \nabla_y \times \mathbf{E}_2(\mathbf{y}) \cdot \mathbf{H}_1(\mathbf{y})\} \ \mathrm{d}\mathbf{y} = \mathbf{0}.
\end{aligned} \tag{A.6}$$

Therefore, for any $\mathbf{q} \in \mathbb{R}^3$ constant, by the second Stratton–Chu formula,

$$\begin{aligned}
\mathbf{q} \cdot \mathbf{E}^s_{pl}(\mathbf{z}, -\widehat{\mathbf{x}}, \mathbf{p}) &= \mathbf{q} \cdot \nabla_z \times \int_{\Gamma_1} (\boldsymbol{\nu}(\mathbf{y}) \times \mathbf{E}^s_{pl}(\mathbf{y}, -\widehat{\mathbf{x}}, \mathbf{p}))\phi(\mathbf{z}, \mathbf{y}) \ \mathrm{d}s(\mathbf{y}) \\
&\quad - \frac{1}{\mathrm{i}k}\mathbf{q} \cdot \nabla_z \times \nabla_z \times \int_{\Gamma_1} (\boldsymbol{\nu}(\mathbf{y}) \times \mathbf{H}^s_{pl}(\mathbf{y}, -\widehat{\mathbf{x}}, \mathbf{p}))\phi(\mathbf{z}, \mathbf{y}) \ \mathrm{d}s(\mathbf{y}) \\
&= \int_{\Gamma_1} (\boldsymbol{\nu}(\mathbf{y}) \times \mathbf{E}^s_{pl}(\mathbf{y}, -\widehat{\mathbf{x}}, \mathbf{p})) \cdot \mathbf{H}^i_{edp}(\mathbf{z}, \mathbf{y}, \mathbf{q}) \ \mathrm{d}s(\mathbf{y}) \\
&\quad + \int_{\Gamma_1} (\boldsymbol{\nu}(\mathbf{y}) \times \mathbf{H}^s_{pl}(\mathbf{y}, -\widehat{\mathbf{x}}, \mathbf{p})) \cdot \mathbf{E}^i_{edp}(\mathbf{z}, \mathbf{y}, \mathbf{q}) \ \mathrm{d}s(\mathbf{y}),
\end{aligned}$$

and if we use (A.5) with $(\mathbf{E}_1, \mathbf{H}_1) = (\mathbf{E}^i_{pl}, \mathbf{H}^i_{pl})$ and $(\mathbf{E}_2, \mathbf{H}_2) = (\mathbf{E}^i_{edp}, \mathbf{H}^i_{edp})$, and (A.6) with $\mathbf{E}_1 = \mathbb{G}^E(\cdot, \mathbf{z})\mathbf{p} - \mathbf{E}^i_{edp}(\mathbf{z}, \cdot, \mathbf{p})$, $\mathbf{H}_1 = \mathbb{G}^H(\cdot, \mathbf{z})\mathbf{p} - \mathbf{H}^i_{edp}(\mathbf{z}, \cdot, \mathbf{p})$ and $(\mathbf{E}_2, \mathbf{H}_2) = (\mathbf{E}_{pl}, \mathbf{H}_{pl})$ we now obtain

$$\begin{aligned}
\mathbf{q} \cdot \mathbf{E}^s_{pl}(\mathbf{z}, -\widehat{\mathbf{x}}, \mathbf{p}) &= \int_{\Gamma_1} (\boldsymbol{\nu}(\mathbf{y}) \times \mathbf{E}_{pl}(\mathbf{y}, -\widehat{\mathbf{x}}, \mathbf{p})) \cdot \mathbf{H}^i_{edp}(\mathbf{z}, \mathbf{y}, \mathbf{q}) \ \mathrm{d}s(\mathbf{y}) \\
&\quad + \int_{\Gamma_1} (\boldsymbol{\nu}(\mathbf{y}) \times \mathbf{H}_{pl}(\mathbf{y}, -\widehat{\mathbf{x}}, \mathbf{p})) \cdot \mathbf{E}^i_{edp}(\mathbf{z}, \mathbf{y}, \mathbf{q}) \ \mathrm{d}s(\mathbf{y}) \\
&\quad - \int_{\Gamma_1} (\boldsymbol{\nu}(\mathbf{y}) \times \mathbf{E}^i_{pl}(\mathbf{y}, -\widehat{\mathbf{x}}, \mathbf{p})) \cdot \mathbf{H}^i_{edp}(\mathbf{z}, \mathbf{y}, \mathbf{q}) \ \mathrm{d}s(\mathbf{y}) \\
&\quad + \int_{\Gamma_1} (\boldsymbol{\nu}(\mathbf{y}) \times \mathbf{H}^i_{pl}(\mathbf{y}, -\widehat{\mathbf{x}}, \mathbf{p})) \cdot \mathbf{E}^i_{edp}(\mathbf{z}, \mathbf{y}, \mathbf{q}) \ \mathrm{d}s(\mathbf{y}), \\
&= \int_{\Gamma_1} (\boldsymbol{\nu}(\mathbf{y}) \times \mathbf{E}_{pl}(\mathbf{y}, -\widehat{\mathbf{x}}, \mathbf{p})) \cdot (\mathbb{G}^H(\mathbf{y}, \mathbf{z})\mathbf{q}) \ \mathrm{d}s(\mathbf{y}) \\
&\quad + \int_{\Gamma_1} (\boldsymbol{\nu}(\mathbf{y}) \times \mathbf{H}_{pl}(\mathbf{y}, -\widehat{\mathbf{x}}, \mathbf{p})) \cdot (\mathbb{G}^E(\mathbf{y}, \mathbf{z})\mathbf{q}) \ \mathrm{d}s(\mathbf{y})
\end{aligned}$$

which finally simplifies to

$$\mathbf{q}\cdot\mathbf{E}^s_{pl}(\mathbf{z},-\widehat{\mathbf{x}},\mathbf{p}) = \int_{\Gamma_1}(\boldsymbol{\nu}(\mathbf{y})\times\mathbb{G}^H(\mathbf{y},\mathbf{z})\mathbf{q})\cdot\mathbf{E}^i_{pl}(\mathbf{y},-\widehat{\mathbf{x}},\mathbf{p})\ \mathrm{d}s(\mathbf{y}) + \int_{\Gamma_1}(\boldsymbol{\nu}(\mathbf{y})\times\mathbb{G}^E(\mathbf{y},\mathbf{z})\mathbf{q})\cdot\mathbf{H}^i_{pl}(\mathbf{y},-\widehat{\mathbf{x}},\mathbf{p})\ \mathrm{d}s(\mathbf{y}). \tag{A.7}$$

Therefore, combining (A.4) and (A.7) yiels

$$4\pi\mathbf{p}\cdot(\mathbb{G}^{E,\infty}(\widehat{\mathbf{x}},\mathbf{z})\mathbf{q}) = \mathbf{q}\cdot\mathbf{E}^i_{pl}(\mathbf{z},-\widehat{\mathbf{x}},\mathbf{p}) + \mathbf{q}\cdot\mathbf{E}^s_{pl}(\mathbf{z},-\widehat{\mathbf{x}},\mathbf{p}) = \mathbf{q}\cdot\mathbf{E}_{pl}(\mathbf{z},-\widehat{\mathbf{x}},\mathbf{p}),$$

for all $\mathbf{z}\in\mathbb{R}^3\setminus\overline{\Omega}$, which completes the proof for this case.

Case 2 . Next let $\mathbf{z}\in\Omega$. Then the field $(\mathbb{G}^E(\cdot,\mathbf{z})\mathbf{q},\mathbb{G}^H(\cdot,\mathbf{z})\mathbf{q})$ is a non-singular radiating solution of the homogeneous Maxwell equations (19) in $\mathbb{R}^3\setminus\overline{\Omega}$, and then taking the dot product of $\mathbf{p}\in\mathbb{R}^3$ with $\mathbb{G}^E(\mathbf{x},\mathbf{z})\mathbf{q}$ and using the Stratton–Chu formula, we have that for any $\mathbf{x}\in\mathbb{R}^3\setminus\overline{\Omega}$,

$$\begin{aligned}\mathbf{p}\cdot\mathbb{G}^E(\mathbf{x},\mathbf{z})\mathbf{q} &= \mathbf{p}\cdot\nabla_x\times\int_{\Gamma_1}(\boldsymbol{\nu}(\mathbf{y})\times\mathbb{G}^E(\mathbf{y},\mathbf{z})\mathbf{q})\phi(\mathbf{x},\mathbf{y})\ \mathrm{d}s(\mathbf{y})\\ &\quad-\frac{1}{\mathrm{i}k}\mathbf{p}\cdot\nabla_x\times\nabla_x\times\int_{\Gamma_1}(\boldsymbol{\nu}(\mathbf{y})\times\mathbb{G}^H(\mathbf{y},\mathbf{z})\mathbf{q})\phi(\mathbf{x},\mathbf{y})\ \mathrm{d}s(\mathbf{y})\\ &= -\int_{\Gamma_1}(\boldsymbol{\nu}(\mathbf{y})\times\mathbb{G}^E(\mathbf{y},\mathbf{z})\mathbf{q})\cdot\nabla_y\times(\phi(\mathbf{x},\mathbf{y})\mathbf{p})\ \mathrm{d}s(\mathbf{y})\\ &\quad-\frac{1}{\mathrm{i}k}\int_{\Gamma_1}(\boldsymbol{\nu}(\mathbf{y})\times\mathbb{G}^H(\mathbf{y},\mathbf{z})\mathbf{q})\cdot\nabla_y\times\nabla_y\times(\phi(\mathbf{x},\mathbf{y})\mathbf{p})\ \mathrm{d}s(\mathbf{y}),\end{aligned}$$

and hence the far field pattern satisfies

$$\begin{aligned}\mathbf{p}\cdot\mathbb{G}^{E,\infty}(\widehat{\mathbf{x}},\mathbf{z})\mathbf{q} =& \frac{1}{4\pi}\int_{\Gamma_1}(\boldsymbol{\nu}(\mathbf{y})\times\mathbb{G}^E(\mathbf{y},\mathbf{z})\mathbf{q})\cdot\mathbf{H}^i_{pl}(\mathbf{y},-\widehat{\mathbf{x}},\mathbf{p})\ \mathrm{d}s(\mathbf{y})\\ &+\frac{1}{4\pi}\int_{\Gamma_1}(\boldsymbol{\nu}(\mathbf{y})\times\mathbb{G}^H(\mathbf{y},\mathbf{z})\mathbf{q})\cdot\mathbf{E}^i_{pl}(\mathbf{y},-\widehat{\mathbf{x}},\mathbf{p})\ \mathrm{d}s(\mathbf{y})\\ =&\frac{1}{4\pi}\int_{\Gamma_1}(\boldsymbol{\nu}(\mathbf{y})\times\mathbb{G}^E(\mathbf{y},\mathbf{z})\mathbf{q})\cdot\mathbf{H}_{pl}(\mathbf{y},-\widehat{\mathbf{x}},\mathbf{p})\ \mathrm{d}s(\mathbf{y})\\ &+\frac{1}{4\pi}\int_{\Gamma_1}(\boldsymbol{\nu}(\mathbf{y})\times\mathbb{G}^H(\mathbf{y},\mathbf{z})\mathbf{q})\cdot\mathbf{E}_{pl}(\mathbf{y},-\widehat{\mathbf{x}},\mathbf{p})\ \mathrm{d}s(\mathbf{y})\\ =&\frac{1}{4\pi}\int_{\Omega}(\nabla_y\times\mathbb{G}^E(\mathbf{y},\mathbf{z})\mathbf{q})\cdot\mathbf{H}_{pl}(\mathbf{y},-\widehat{\mathbf{x}},\mathbf{p})\ \ \mathrm{d}\mathbf{y}\\ &-\frac{1}{4\pi}\int_{\Omega}(\nabla_y\times\mathbf{H}_{pl}(\mathbf{y},-\widehat{\mathbf{x}},\mathbf{p}))\cdot\mathbb{G}^E(\mathbf{y},\mathbf{z})\mathbf{q}\ \ \mathrm{d}\mathbf{y}\\ &+\frac{1}{4\pi}\int_{\Omega}(\nabla_y\times\mathbb{G}^H(\mathbf{y},\mathbf{z})\mathbf{q})\cdot\mathbf{E}_{pl}(\mathbf{y},-\widehat{\mathbf{x}},\mathbf{p})\ \ \mathrm{d}\mathbf{y}\\ &-\frac{1}{4\pi}\int_{\Omega}(\nabla_y\times\mathbf{E}_{pl}(\mathbf{y},-\widehat{\mathbf{x}},\mathbf{p}))\cdot\mathbb{G}^H(\mathbf{y},\mathbf{z})\mathbf{q}\ \ \mathrm{d}\mathbf{y},\end{aligned}$$

where in the second equality we have used the fact that for every two radiating solutions of (19) in $\mathbb{R}^3\setminus\overline{\Omega}$, $(\mathbf{E}^s_1,\mathbf{H}^s_1)$ and $(\mathbf{E}^s_2,\mathbf{H}^s_2)$ the following holds

$$0 = \int_{\Gamma_1} \{(\boldsymbol{\nu}(\mathbf{y}) \times \mathbf{E}_1^s) \cdot \mathbf{H}_2^s + (\boldsymbol{\nu}(\mathbf{y}) \times \mathbf{H}_1^s) \cdot \mathbf{E}_2^s\} \ \mathrm{d}s(\mathbf{y}). \tag{A.8}$$

Therefore, from (A.8) we obtain the desired result

$$\begin{aligned}\mathbf{p} \cdot \mathbb{G}^{E,\infty}(\widehat{\mathbf{x}}, \mathbf{z})\mathbf{q} = \frac{1}{4\pi} \int_\Omega \mathrm{i}k\mu(\mathbb{G}^H(\mathbf{y}, \mathbf{z})\mathbf{q}) \cdot \mathbf{H}_{pl}(\mathbf{y}, -\widehat{\mathbf{x}}, \mathbf{p}) \ \ \mathrm{d}\,\mathbf{y} \\ + \frac{1}{4\pi} \int_\Omega \mathrm{i}k\epsilon \mathbf{E}_{pl}(\mathbf{y}, -\widehat{\mathbf{x}}, \mathbf{p}) \cdot \mathbb{G}^E(\mathbf{y}, \mathbf{z})\mathbf{q} \ \ \mathrm{d}\,\mathbf{y} \\ + \frac{1}{4\pi} \int_\Omega (-\mathrm{i}k\epsilon \mathbb{G}^E(\mathbf{y}, \mathbf{z})\mathbf{q} + \mathbf{q}\delta(\mathbf{y} - \mathbf{z})) \cdot \mathbf{E}_{pl}(\mathbf{y}, -\widehat{\mathbf{x}}, \mathbf{p}) \ \ \mathrm{d}\,\mathbf{y} \\ - \frac{1}{4\pi} \int_\Omega \mathrm{i}k\mu \mathbf{H}_{pl}(\mathbf{y}, -\widehat{\mathbf{x}}, \mathbf{p}) \cdot \mathbb{G}^H(\mathbf{y}, \mathbf{z})\mathbf{q} \ \ \mathrm{d}\,\mathbf{y} = \frac{1}{4\pi}\mathbf{q} \cdot \mathbf{E}_{pl}(\mathbf{z}, -\widehat{\mathbf{x}}, \mathbf{p}).\end{aligned}$$

Case 3. Lastly we consider $\mathbf{z} \in \Gamma_1 \cup \Gamma$. Notice that by continuity of the tangential traces of $\mathbf{E}_{pl}(\cdot, -\widehat{\mathbf{x}}, \mathbf{p})$ and $\mathbb{G}^{E,\infty}(\widehat{\mathbf{x}}, \cdot)\mathbf{p}$ accross $\Gamma_1 \cup \Gamma$, the identity (22) is true at $\mathbf{z} \in \Gamma_1 \cup \Gamma$ as long as $\mathbf{p}, \mathbf{q} \in \mathbb{R}^3$ satisfy $\boldsymbol{\nu}(\mathbf{z}) \cdot \mathbf{p} = \boldsymbol{\nu}(\mathbf{z}) \cdot \mathbf{q} = 0$, and the proof is complete.

Appendix B. Proof of theorem 3.2

Proof. Following the arguments of the proof of theorem 6.30 in [10], if $\widehat{\mathbf{x}}, \widehat{\mathbf{d}} \in \mathbb{S}^2$ and $\mathbf{p}, \mathbf{q} \in \mathbb{R}^3$, then from the divergence theorem in Ω,

$$\begin{aligned}0 &= \int_{(\Gamma \setminus \Gamma_0) \cup \Gamma_+} \boldsymbol{\nu}(\mathbf{y}) \times \mathbf{E}_{pl}^i(\mathbf{y}, \widehat{\mathbf{d}}, \mathbf{p}) \cdot \mathbf{H}_{pl}^i(\mathbf{y}, -\widehat{\mathbf{x}}, \mathbf{q}) \ \ \mathrm{d}s(\mathbf{y}) \\ &= \int_{(\Gamma \setminus \Gamma_0) \cup \Gamma_+} \boldsymbol{\nu}(\mathbf{y}) \times \mathbf{H}_{pl}^i(\mathbf{y}, \widehat{\mathbf{d}}, \mathbf{p}) \cdot \mathbf{E}_{pl}^i(\mathbf{y}, -\widehat{\mathbf{x}}, \mathbf{q}) \ \ \mathrm{d}s(\mathbf{y}),\end{aligned} \tag{B.1}$$

and from the radiation condition we have that $(\mathbf{E}_{pl}^s(\cdot, \widehat{\mathbf{d}}, \mathbf{p}), \mathbf{H}_{pl}^s(\cdot, \widehat{\mathbf{d}}, \mathbf{p}))$ and $(\mathbf{E}_{pl}^s(\cdot, -\widehat{\mathbf{x}}, \mathbf{q}), \mathbf{H}_{pl}^s(\cdot, -\widehat{\mathbf{x}}, q))$ satisfy

$$\begin{aligned}0 = \int_{(\Gamma \setminus \Gamma_0) \cup \Gamma_+} &\boldsymbol{\nu}(\mathbf{y}) \times \mathbf{E}_{pl}^s(\mathbf{y}, \widehat{\mathbf{d}}, \mathbf{p}) \cdot \mathbf{H}_{pl}^s(\mathbf{y}, -\widehat{\mathbf{x}}, \mathbf{q}) \\ &+ \boldsymbol{\nu}(\mathbf{y}) \times \mathbf{H}_{pl}^s(\mathbf{y}, \widehat{\mathbf{d}}, \mathbf{p}) \cdot \mathbf{E}_{pl}^s(\mathbf{y}, -\widehat{\mathbf{x}}, \mathbf{q}) \ \ \mathrm{d}s(\mathbf{y}).\end{aligned} \tag{B.2}$$

Moreover,

$$\begin{aligned}4\pi\mathbf{q} \cdot \mathbf{E}_{pl}^\infty(\widehat{\mathbf{x}}, \widehat{\mathbf{d}}, \mathbf{p}) = \int_{(\Gamma \setminus \Gamma_0) \cup \Gamma_+} &\boldsymbol{\nu}(\mathbf{y}) \times \mathbf{E}_{pl}^s(\mathbf{y}, \widehat{\mathbf{d}}, \mathbf{p}) \cdot \mathbf{H}_{pl}^i(\mathbf{y}, -\widehat{\mathbf{x}}, \mathbf{q}) \\ &+ \boldsymbol{\nu}(\mathbf{y}) \times \mathbf{H}_{pl}^s(\mathbf{y}, \widehat{\mathbf{d}}, \mathbf{p}) \cdot \mathbf{E}_{pl}^i(\mathbf{y}, -\widehat{\mathbf{x}}, \mathbf{q}) \ \ \mathrm{d}s(\mathbf{y})\end{aligned} \tag{B.3}$$

and

$$\begin{aligned}4\pi\mathbf{p} \cdot \mathbf{E}_{pl}^\infty(-\widehat{\mathbf{d}}, -\widehat{\mathbf{x}}, \mathbf{q}) = \int_{(\Gamma \setminus \Gamma_0) \cup \Gamma_+} &\boldsymbol{\nu}(\mathbf{y}) \times \mathbf{E}_{pl}^s(\mathbf{y}, -\widehat{\mathbf{x}}, \mathbf{q}) \cdot \mathbf{H}_{pl}^i(\mathbf{y}, \widehat{\mathbf{d}}, \mathbf{p}) \\ &+ \boldsymbol{\nu}(\mathbf{y}) \times \mathbf{H}_{pl}^s(\mathbf{y}, -\widehat{\mathbf{x}}, \mathbf{q}) \cdot \mathbf{E}_{pl}^i(\mathbf{y}, \widehat{\mathbf{d}}, \mathbf{p}) \ \ \mathrm{d}s(\mathbf{y}),\end{aligned} \tag{B.4}$$

and therefore considering the sum (B.1)–(B.4) we get,

$$\begin{aligned}
&4\pi(\mathbf{q}\cdot\mathbf{E}_{pl}^{\infty}(\widehat{\mathbf{x}},\widehat{\mathbf{d}},\mathbf{p})-\mathbf{p}\cdot\mathbf{E}_{pl}^{\infty}(-\widehat{\mathbf{d}},-\widehat{\mathbf{x}},\mathbf{q}))\\
&=\int_{(\Gamma\setminus\Gamma_0)\cup\Gamma_+}\boldsymbol{\nu}(\mathbf{y})\times\mathbf{E}_{pl}(\mathbf{y},-\widehat{\mathbf{x}},\mathbf{q})\cdot\mathbf{H}_{pl}(\mathbf{y},\widehat{\mathbf{d}},\mathbf{p})\ \mathrm{d}s(\mathbf{y})\\
&\quad+\int_{(\Gamma\setminus\Gamma_0)\cup\Gamma_+}\boldsymbol{\nu}(\mathbf{y})\times\mathbf{H}_{pl}(\mathbf{y},-\widehat{\mathbf{x}},\mathbf{q})\cdot\mathbf{E}_{pl}(\mathbf{y},\widehat{\mathbf{d}},\mathbf{p})\ \mathrm{d}s(\mathbf{y}).
\end{aligned}$$

Splitting the above as sum of integrals over Γ_+ and G_- and using the continuity of the tangential component of the electric and magnetic fields across $\Gamma=\Gamma\setminus\Gamma_0$ we obtain

$$\begin{aligned}
&4\pi(\mathbf{q}\cdot\mathbf{E}_{pl}^{\infty}(\widehat{\mathbf{x}},\widehat{\mathbf{d}},\mathbf{p})-\mathbf{p}\cdot\mathbf{E}_{pl}^{\infty}(-\widehat{\mathbf{d}},-\widehat{\mathbf{x}},\mathbf{q}))\\
&=\int_{\Gamma_0}[\![\boldsymbol{\nu}(\mathbf{y})\times\mathbf{E}_{pl}(\mathbf{y},-\widehat{\mathbf{x}},\mathbf{q})]\!]\cdot\langle\!\langle\mathbf{H}_{pl}(\mathbf{y},\widehat{\mathbf{d}},\mathbf{p})\rangle\!\rangle\ \mathrm{d}s(\mathbf{y})\\
&\quad+\int_{\Gamma_0}[\![\boldsymbol{\nu}(\mathbf{y})\times\mathbf{H}_{pl}(\mathbf{y},-\widehat{\mathbf{x}},\mathbf{q})]\!]\cdot\langle\!\langle\mathbf{E}_{pl}(\mathbf{y},\widehat{\mathbf{d}},\mathbf{p})\rangle\!\rangle\ \mathrm{d}s(\mathbf{y})\\
&\quad-\int_{\Gamma_0}\langle\!\langle\mathbf{E}_{pl}(\mathbf{y},-\widehat{\mathbf{x}},\mathbf{q})\rangle\!\rangle\cdot[\![\boldsymbol{\nu}(\mathbf{y})\times\mathbf{H}_{pl}(\mathbf{y},\widehat{\mathbf{d}},\mathbf{p})]\!]\ \mathrm{d}s(\mathbf{y})\\
&\quad+\int_{\Gamma_0}\langle\!\langle\mathbf{H}_{pl}(\mathbf{y},-\widehat{\mathbf{x}},\mathbf{q})\rangle\!\rangle\cdot[\![\boldsymbol{\nu}(\mathbf{y})\times\mathbf{E}_{pl}(\mathbf{y},\widehat{\mathbf{d}},\mathbf{p})]\!]\ \mathrm{d}s(\mathbf{y})
\end{aligned}$$

which by substituting the expression (5) and (6) for the ATCs of our approximate model, implies that

$$\begin{aligned}
&4\pi(\mathbf{q}\cdot\mathbf{E}_{pl}^{\infty}(\widehat{\mathbf{x}},\widehat{\mathbf{d}},\mathbf{p})-\mathbf{p}\cdot\mathbf{E}_{pl}^{\infty}(-\widehat{\mathbf{d}},-\widehat{\mathbf{x}},\mathbf{q}))\\
&\quad=\int_{\Gamma_0}\mathrm{i}k\delta\mathcal{A}_1\langle\!\langle(\mathbf{H}_{pl}(\mathbf{y},-\widehat{\mathbf{x}},\mathbf{q}))_T\rangle\!\rangle\cdot\langle\!\langle(\mathbf{H}_{pl}(\mathbf{y},\widehat{\mathbf{d}},\mathbf{p}))_T\rangle\!\rangle\ \mathrm{d}s(\mathbf{y})\\
&\qquad+\int_{\Gamma_0}\frac{\delta}{\mathrm{i}k}\mathcal{A}_2\langle\!\langle(\mathbf{E}_{pl}(\mathbf{y},-\widehat{\mathbf{x}},\mathbf{q}))_T\rangle\!\rangle\cdot\langle\!\langle(\mathbf{E}_{pl}(\mathbf{y},\widehat{\mathbf{d}},\mathbf{p}))_T\rangle\!\rangle\ \mathrm{d}s(\mathbf{y})\\
&\qquad-\int_{\Gamma_0}\langle\!\langle(\mathbf{E}_{pl}(\mathbf{y},-\widehat{\mathbf{x}},\mathbf{q}))_T\rangle\!\rangle\cdot\frac{\delta}{\mathrm{i}k}\mathcal{A}_2\langle\!\langle(\mathbf{E}_{pl}(\mathbf{y},\widehat{\mathbf{d}},\mathbf{p}))_T\rangle\!\rangle\ \mathrm{d}s(\mathbf{y})\\
&\qquad+\int_{\Gamma_0}\langle\!\langle(\mathbf{H}_{pl}(\mathbf{y},-\widehat{\mathbf{x}},\mathbf{q}))_T\rangle\!\rangle\cdot\mathrm{i}k\delta\mathcal{A}_1\langle\!\langle(\mathbf{H}_{pl}(\mathbf{y},\widehat{\mathbf{d}},\mathbf{p}))_T\rangle\!\rangle\ \mathrm{d}s(\mathbf{y})=0,
\end{aligned}$$

where $\mathcal{A}_i$, $i=1,2$ are defined by (2) (here we have used the fact that $\mathcal{A}_i$ are symmetric in the duality pairing with L^2-pivot space, i.e. without conjugation). □

Appendix C. Proof of proposition 3.1

Proof. Observe first that by linearity,

$$\mathbf{E}_{b,\mathbf{g}}(\mathbf{x})=\int_{\mathbb{S}^2}\mathbf{E}_{pl}(\mathbf{x},\widehat{\mathbf{d}},\mathbf{g}(\widehat{\mathbf{d}}))\ \ \mathrm{d}s(\widehat{\mathbf{d}}),$$

and thanks to theorem 3.1, for all $\mathbf{p}\in\mathbb{R}^3$,

$$\mathbf{p}\cdot\mathbf{E}_{b,\mathbf{g}}(\mathbf{x}) = \int_{\mathbb{S}^2} 4\pi\mathbf{g}(\widehat{\mathbf{d}})\cdot\mathbb{G}^{E,\infty}(-\widehat{\mathbf{d}},\mathbf{x})\mathbf{p}\ \ \mathrm{d}s(\widehat{\mathbf{d}}).$$

Observe that

$$\mathbf{H}(\mathrm{curl}_\Gamma,\Gamma_0) \ = \left\{\nabla_\Gamma p+\nabla_\Gamma\times q\,\middle|\,\nabla_\Gamma\times q\in\mathbf{H}_t^1(\Gamma_0),\ \nabla_\Gamma p\in\mathbf{L}_t^2(\Gamma_0)\right\}$$

and thus

$$\begin{aligned}\mathbf{H}(\mathrm{curl}_\Gamma,\Gamma_0)^* &= \left\{\nabla_\Gamma p+\nabla_\Gamma\times q\,\middle|\,\nabla_\Gamma\times q\in\mathbf{H}_0^{-1}(\Gamma_0),\ \nabla_\Gamma p\in\mathbf{L}_t^2(\Gamma_0)\right\},\\ &= \mathbf{H}_0^{-1}(\mathrm{div}_\Gamma,\Gamma_0).\end{aligned}$$

Given $(\boldsymbol{\xi},\boldsymbol{\eta},\boldsymbol{\sigma})\in\mathbf{H}_0^{-1}(\mathrm{div}_\Gamma,\Gamma_0)\times\mathcal{H}_0(\Gamma_0)\times\tilde{\mathbf{H}}^{-1/2}(\mathrm{curl}_{\mathscr{S}},\mathscr{S})$, where $\langle\cdot,\cdot\rangle$ denotes duality pairing with pivoting space $\mathbf{L}_t^2$ (on either Γ_0 or $\mathscr{S}$), we can write

$$\begin{aligned}\langle\mathscr{H}\mathbf{g},\,(\boldsymbol{\xi},\boldsymbol{\eta},\boldsymbol{\sigma})\rangle = &\int_{\Gamma_0}\left\{\delta\langle\!\langle(\mu^{-1}\nabla\times\mathbf{E}_{b,\mathbf{g}})_T\rangle\!\rangle\cdot\overline{\boldsymbol{\xi}}-\mathcal{A}_1^{-1}[\![\boldsymbol{\nu}\times\mathbf{E}_{b,\mathbf{g}}]\!]\cdot\overline{\boldsymbol{\xi}}\right\}\ \mathrm{d}s(\mathbf{y})\\ &+\int_{\Gamma_0}\left\{\delta\mathcal{A}_2\langle\!\langle(\mathbf{E}_{b,\mathbf{g}})_T\rangle\!\rangle\cdot\overline{\boldsymbol{\eta}}-[\![\boldsymbol{\nu}\times(\mu^{-1}\nabla\times\mathbf{E}_{b,\mathbf{g}})]\!]\cdot\overline{\boldsymbol{\eta}}\right\}\ \mathrm{d}s(\mathbf{y})\\ &-\int_{\mathscr{S}}\mathbf{n}\times\left(\mu^{-1}\nabla\times\mathbf{E}_{b,\mathbf{g}}\right)\cdot\overline{\boldsymbol{\sigma}}\ \ \mathrm{d}s(\mathbf{y}).\end{aligned}$$

Substituting the expression for $\mathbf{E}_b$

$$\begin{aligned}\langle\mathscr{H}\mathbf{g},\,(\boldsymbol{\xi},\boldsymbol{\eta},\boldsymbol{\sigma})\rangle = &\int_{\Gamma_0}\int_{\mathbb{S}^2}\Big\{\delta\langle\!\langle(\mu^{-1}\nabla\times\mathbf{E}_b(\mathbf{y},\widehat{\mathbf{d}},\mathbf{g}(\widehat{\mathbf{d}}))_T\rangle\!\rangle\ \cdot\ \overline{\boldsymbol{\xi}}\\ &-\mathcal{A}_1^{-1}[\![\boldsymbol{\nu}\times\mathbf{E}_b(\mathbf{y},\widehat{\mathbf{d}},\mathbf{g}(\widehat{\mathbf{d}}))]\!]\cdot\overline{\boldsymbol{\xi}}\Big\}\ \mathrm{d}s(\widehat{\mathbf{d}})\ \mathrm{d}s(\mathbf{y})\\ &+\int_{\Gamma_0}\int_{\mathbb{S}^2}\Big\{\delta\mathcal{A}_2\langle\!\langle(\mathbf{E}_b(\mathbf{y},\widehat{\mathbf{d}},\mathbf{g}(\widehat{\mathbf{d}})))_T\rangle\!\rangle\cdot\overline{\boldsymbol{\eta}}\\ &-[\![\boldsymbol{\nu}\times(\mu^{-1}\nabla\times\mathbf{E}_b(\mathbf{y},\widehat{\mathbf{d}},\mathbf{g}(\widehat{\mathbf{d}})))]\!]\cdot\overline{\boldsymbol{\eta}}\Big\}\ \mathrm{d}s(\widehat{\mathbf{d}})\ \mathrm{d}s(\mathbf{y})\\ &-\int_{\mathscr{S}}\int_{\mathbb{S}^2}\Big(\mathbf{n}\times(\mu^{-1}\nabla\times\mathbf{E}_b(\mathbf{y},\widehat{\mathbf{d}},\mathbf{g}(\widehat{\mathbf{d}})))\Big)\cdot\overline{\boldsymbol{\sigma}}\ \ \mathrm{d}s(\widehat{\mathbf{d}})\ \ \mathrm{d}s(\mathbf{y}).\end{aligned}$$

Then by the mixed reciprocity principle (theorem 3.1),

$$\begin{aligned}\frac{1}{4\pi}\langle\mathscr{H}\mathbf{g},\,(\boldsymbol{\xi},\boldsymbol{\eta},\boldsymbol{\sigma})\rangle = &\int_{\mathbb{S}^2}\mathbf{g}(\widehat{\mathbf{d}})\cdot\Bigg\{\int_{\Gamma_0}\Big\{\delta\langle\!\langle(\mu^{-1}\nabla\times\mathbb{G}^{E,\infty}(-\widehat{\mathbf{d}},\mathbf{y}))_T\rangle\!\rangle\,\overline{\boldsymbol{\xi}(\mathbf{y})}\\ &+[\![\mathbb{G}^{E,\infty}(-\widehat{\mathbf{d}},\mathbf{y})]\!](\boldsymbol{\nu}\times\mathcal{A}_1^{-1}\overline{\boldsymbol{\xi}(\mathbf{y})})\Big\}\ \mathrm{d}s(\mathbf{y})+\int_{\Gamma_0}\Big\{\delta\langle\!\langle(\mathbb{G}^{E,\infty}(-\widehat{\mathbf{d}},\mathbf{y}))_T\rangle\!\rangle\mathcal{A}_2\overline{\boldsymbol{\eta}(\mathbf{y})}\\ &+[\![(\mu^{-1}\nabla\times\mathbb{G}^{E,\infty}(-\widehat{\mathbf{d}},\mathbf{y}))_T]\!](\boldsymbol{\nu}\times\overline{\boldsymbol{\eta}(\mathbf{y})})\Big\}\ \mathrm{d}s(\mathbf{y})\\ &+\int_{\mathscr{S}}\mu^{-1}\nabla\times\mathbb{G}^{E,\infty}(-\widehat{\mathbf{d}},\mathbf{y})(\mathbf{n}\times\overline{\boldsymbol{\sigma}(\mathbf{y})})\ \ \mathrm{d}s(\mathbf{y})\Bigg\}\ \mathrm{d}s(\widehat{\mathbf{d}}),\end{aligned}$$

where $(\mathbb{G}^{E,\infty}(\cdot,\cdot))_T\mathbf{v} := (\mathbb{G}^{E,\infty})(\cdot,\cdot)\mathbf{v})_T$ for any $\mathbf{v}\in\mathbb{R}^3$.

Notice that in general $\mathcal{A}_1^{-1}$ and $\mathcal{A}_2$ are not self-adjoint operators because $\Im(\epsilon_\delta) > 0$. Letting

$$\overline{\mathcal{A}_1}\boldsymbol{\eta} := \overline{\alpha_1}\boldsymbol{\eta} - \overline{\beta_1}\overrightarrow{\mathrm{curl}_\Gamma}\,\mathrm{curl}_\Gamma\,\boldsymbol{\eta}, \quad \text{and} \quad \overline{\mathcal{A}_2}\boldsymbol{\eta} := \overline{\alpha_2}\boldsymbol{\eta} - \overline{\beta_2}\overrightarrow{\mathrm{curl}_\Gamma}\,\mathrm{curl}_\Gamma\,\boldsymbol{\eta},$$

we can conclude that the conjugate transpose operator $\mathscr{H}^* : \mathbf{H}^{-1/2}(\mathrm{curl}_\Gamma,\Gamma_0)\times \mathbf{H}^{-1/2}(\mathrm{curl}_\Gamma,\Gamma_0) \to \mathbf{L}_t^2(\mathbb{S}^2)$ of $\mathscr{H}$, is given by:

$$\begin{aligned}\frac{1}{4\pi}\mathscr{H}^*(\boldsymbol{\xi},\boldsymbol{\eta},\boldsymbol{\sigma}) = \int_{\Gamma_0} \Big\{ & \delta\overline{\langle\!\langle(\mu^{-1}\nabla\times\mathbb{G}^{E,\infty}(-\cdot,\mathbf{y}))_T\rangle\!\rangle}\,\boldsymbol{\xi}(\mathbf{y}) \\ & + \overline{[\![\mathbb{G}^{E,\infty}(-\cdot,\mathbf{y})]\!]}(\boldsymbol{\nu}\times\overline{\mathcal{A}_1}^{-1}\boldsymbol{\xi}(\mathbf{y}))\Big\}\ \mathrm{d}s(\mathbf{y}) \\ & + \int_{\Gamma_0}\Big\{\delta\overline{\langle\!\langle(\mathbb{G}^{E,\infty}(-\cdot,\mathbf{y}))_T\rangle\!\rangle}\ \overline{\mathcal{A}_2}\boldsymbol{\eta}(\mathbf{y}) \\ & + \overline{[\![(\mu^{-1}\nabla\times\mathbb{G}^{E,\infty}(-\cdot,\mathbf{y}))_T]\!]}(\boldsymbol{\nu}\times\boldsymbol{\eta}(\mathbf{y}))\Big\}\ \mathrm{d}s(\mathbf{y}) \\ & + \int_{\mathscr{S}}\overline{\mu^{-1}\nabla\times\mathbb{G}^{E,\infty}(-\cdot,\mathbf{y})}(\mathbf{n}\times\boldsymbol{\sigma}(\mathbf{y}))\ \mathrm{d}s(\mathbf{y}).\end{aligned}$$

Thus $\mathbf{E}^\infty(\widehat{\mathbf{x}}) = \frac{1}{4\pi}\overline{\mathscr{H}^*(\boldsymbol{\xi},\boldsymbol{\eta},\boldsymbol{\sigma})}(-\widehat{\mathbf{x}})$ is the far field pattern of the following potential:

$$\begin{aligned}\mathbf{E}(\mathbf{x}) = \int_{\Gamma_0}\Big\{ & \delta\langle\!\langle(\mu^{-1}\nabla\times\mathbb{G}^E(\mathbf{x},\mathbf{y}))_T\rangle\!\rangle\,\overline{\boldsymbol{\xi}(\mathbf{y})} \\ & + [\![\mathbb{G}^E(\mathbf{x},\mathbf{y})]\!]\left(\boldsymbol{\nu}\times(\overline{\mathcal{A}_1}^{-1}\overline{\boldsymbol{\xi}(\mathbf{y})})\right)\Big\}\ \mathrm{d}s(\mathbf{y}) \\ & + \int_{\Gamma_0}\Big\{\delta\langle\!\langle(\mathbb{G}^E(\mathbf{x},\mathbf{y}))_T\rangle\!\rangle\overline{\mathcal{A}_2}\,\overline{\boldsymbol{\eta}(\mathbf{y})} \\ & + [\![(\mu^{-1}\nabla\times\mathbb{G}^E(\mathbf{x},\mathbf{y}))_T]\!](\boldsymbol{\nu}\times\overline{\boldsymbol{\eta}(\mathbf{y})})\Big\}\ \mathrm{d}s(\mathbf{y}) \\ & + \int_{\mathscr{S}}\mu^{-1}\nabla\times\mathbb{G}^E(\mathbf{x},\mathbf{y})(\mathbf{n}\times\overline{\boldsymbol{\sigma}(\mathbf{y})})\ \mathrm{d}s(\mathbf{y}).\end{aligned}$$

Observe that $\mathbf{E} = (\mathbf{E}_{\Gamma_+})_T + (\mathbf{E}_{\Gamma_-})_T + \mathbf{E}_{\mathscr{S}}$, where we define

$$\begin{aligned}\mathbf{E}_{\Gamma_+}(\mathbf{x}) := \int_{\Gamma_0}\Big\{ & \frac{\delta}{2}\mu_+^{-1}\nabla\times\mathbb{G}^E(\mathbf{x},\mathbf{y}_\Gamma+\delta f^+\boldsymbol{\nu})\,\overline{\boldsymbol{\xi}(\mathbf{y}_\Gamma)} \\ & + \mathbb{G}^E(\mathbf{x},\mathbf{y}_\Gamma+\delta f^+\boldsymbol{\nu})(\boldsymbol{\nu}\times\overline{\mathcal{A}_1}^{-1}\overline{\boldsymbol{\xi}(\mathbf{y}_\Gamma)})\Big\}\ \mathrm{d}\,\mathbf{y}_\Gamma \\ & + \int_{\Gamma_0}\Big\{\frac{\delta}{2}\mathbb{G}^E(\mathbf{x},\mathbf{y}_\Gamma+\delta f^+\boldsymbol{\nu})\overline{\mathcal{A}_2}\overline{\boldsymbol{\eta}(\mathbf{y}_\Gamma)} \\ & + \mu_+^{-1}\nabla\times\mathbb{G}^E(\mathbf{x},\mathbf{y}_\Gamma+\delta f^+\boldsymbol{\nu})(\boldsymbol{\nu}\times\overline{\boldsymbol{\eta}(\mathbf{y}_\Gamma)})\Big\}\ \mathrm{d}\,\mathbf{y}_\Gamma,\end{aligned}$$

$$\begin{aligned}\mathbf{E}_{\Gamma_-}(\mathbf{x}) := \int_{\Gamma_0} \Big\{ &\frac{\delta}{2}\mu_-^{-1}\nabla\times\mathbb{G}^E(\mathbf{x},\mathbf{y}_\Gamma-\delta f^-\boldsymbol{\nu})\,\overline{\boldsymbol{\xi}(\mathbf{y}_\Gamma)}\\ &-\mathbb{G}^E(\mathbf{x},\mathbf{y}_\Gamma-\delta f^-\boldsymbol{\nu})(\boldsymbol{\nu}\times\overline{\mathcal{A}_1}^{-1}\overline{\boldsymbol{\xi}(\mathbf{y}_\Gamma)})\Big\}\,\mathrm{d}\,\mathbf{y}_\Gamma\\ &+\int_{\Gamma_0}\Big\{\frac{\delta}{2}\mathbb{G}^E(\mathbf{x},\mathbf{y}_\Gamma-\delta f^-\boldsymbol{\nu})\overline{\mathcal{A}_2}\overline{\boldsymbol{\eta}(\mathbf{y}_\Gamma)}\\ &-\mu_-^{-1}\nabla\times\mathbb{G}^E(\mathbf{x},\mathbf{y}_\Gamma-\delta f^-\boldsymbol{\nu})(\boldsymbol{\nu}\times\overline{\boldsymbol{\eta}(\mathbf{y}_\Gamma)})\Big\}\,\mathrm{d}\,\mathbf{y}_\Gamma,\end{aligned}$$

$$\mathbf{E}_{\mathscr{S}}(\mathbf{x}) := \int_{\mathscr{S}} \mu^{-1}\nabla\times\mathbb{G}^E(\mathbf{x},\mathbf{y})(\mathbf{n}\times\overline{\boldsymbol{\sigma}(\mathbf{y})})\;\mathrm{d}s(\mathbf{y}).$$

Moreover, using the notation and the representation formula in remark 3.1, along with jump relations of the electric and magnetic potentials across Γ_-, Γ_+, and $\mathscr{S}$ we obtain

$$\begin{aligned}[\boldsymbol{\nu}\times\mathbf{E}]_{\Gamma_+} &= \left[\boldsymbol{\nu}\times\mathbf{E}_{\Gamma_+}\right]_{\Gamma_+} = -\mathrm{i}k\frac{\delta}{2}\overline{\boldsymbol{\xi}} - \mathrm{i}k(\boldsymbol{\nu}\times\overline{\boldsymbol{\eta}}),\\ [\boldsymbol{\nu}\times\mathbf{E}]_{\Gamma_-} &= \left[\boldsymbol{\nu}\times\mathbf{E}_{\Gamma_-}\right]_{\Gamma_-} = -\mathrm{i}k\frac{\delta}{2}\overline{\boldsymbol{\xi}} + \mathrm{i}k(\boldsymbol{\nu}\times\overline{\boldsymbol{\eta}}),\\ [\boldsymbol{\nu}\times\mathbf{E}]_{\mathscr{S}} &= [\boldsymbol{\nu}\times\mathbf{E}_{\mathscr{S}}]_{\mathscr{S}} = -\mathrm{i}k(\mathbf{n}\times\overline{\boldsymbol{\sigma}}),\end{aligned} \tag{C.1}$$

and

$$\begin{aligned}\left[\boldsymbol{\nu}\times\left(\mu^{-1}\nabla\times\mathbf{E}\right)\right]_{\Gamma_+} &= \left[\boldsymbol{\nu}\times\left(\mu^{-1}\nabla\times\mathbf{E}_{\Gamma_+}\right)\right]_{\Gamma_+} = \mathrm{i}k(\boldsymbol{\nu}\times\overline{\mathcal{A}_1}^{-1}\overline{\boldsymbol{\xi}}) + \mathrm{i}k\frac{\delta}{2}\overline{\mathcal{A}_2}\overline{\boldsymbol{\eta}},\\ \left[\boldsymbol{\nu}\times\left(\mu^{-1}\nabla\times\mathbf{E}\right)\right]_{\Gamma_-} &= \left[\boldsymbol{\nu}\times\left(\mu^{-1}\nabla\times\mathbf{E}_{\Gamma_-}\right)\right]_{\Gamma_-} = -\mathrm{i}k(\boldsymbol{\nu}\times\overline{\mathcal{A}_1}^{-1}\overline{\boldsymbol{\xi}}) + \mathrm{i}k\frac{\delta}{2}\overline{\mathcal{A}_2}\overline{\boldsymbol{\eta}},\\ \left[\mathbf{n}\times\left(\mu^{-1}\nabla\times\mathbf{E}\right)\right]_{\mathscr{S}} &= \left[\mathbf{n}\times\left(\mu^{-1}\nabla\times\mathbf{E}_{\mathscr{S}}\right)\right]_{\mathscr{S}} = \mathbf{0}.\end{aligned} \tag{C.2}$$

Now, suppose then that $\mathbf{E}^\infty = \mathbf{0}$, then by the Rellich lemma (lemma 9.28 in [21]), we know that $\mathbf{E} = \mathbf{0}$ in $\mathbb{R}^3\setminus\overline{\Omega}$. Moreover, from the assumptions of $|\nabla\mu|$ and the unique continuation principle for isotropic time harmonic Maxwell equations (theorem 2.3 in [24]) combined with Holmgren's uniqueness type theorem, we ensure that $\mathbf{E} = \mathbf{0}$ in $\mathbb{R}^3\setminus\overline{\Omega}_\delta$. Then

$$[\boldsymbol{\nu}\times\mathbf{E}]_{\Gamma_+} = \boldsymbol{\nu}\times\mathbf{E}^{out}\Big|_{\Gamma_+} - \boldsymbol{\nu}\times\mathbf{E}^{\delta}\Big|_{\Gamma_+} = -\boldsymbol{\nu}\times\mathbf{E}^{\delta}\Big|_{\Gamma_+}, \tag{C.3}$$

$$[\boldsymbol{\nu}\times\mathbf{E}]_{\Gamma_-} = \boldsymbol{\nu}\times\mathbf{E}^{\delta}\Big|_{\Gamma_-} - \boldsymbol{\nu}\times\mathbf{E}^{out}\Big|_{\Gamma_-} = \boldsymbol{\nu}\times\mathbf{E}^{\delta}\Big|_{\Gamma_-}, \tag{C.4}$$

$$[\boldsymbol{\nu}\times\mathbf{E}]_{\mathscr{S}} = \mathbf{n}\times\mathbf{E}^{out}\Big|_{\mathscr{S}} - \mathbf{n}\times\mathbf{E}^{\delta}\Big|_{\mathscr{S}} = -\mathbf{n}\times\mathbf{E}^{\delta}\Big|_{\mathscr{S}}, \tag{C.5}$$

and

$$\begin{aligned}\left[\boldsymbol{\nu}\times\left(\mu^{-1}\nabla\times\mathbf{E}\right)\right]_{\Gamma_+} &= \boldsymbol{\nu}\times(\mu^{-1}\nabla\times\mathbf{E}^{out})\Big|_{\Gamma_+} - \boldsymbol{\nu}\times\left(\mu^{-1}\nabla\times\mathbf{E}^{\delta}\right)\Big|_{\Gamma_+}\\ &= -\boldsymbol{\nu}\times\left(\mu^{-1}\nabla\times\mathbf{E}^{\delta}\right)\Big|_{\Gamma_+},\end{aligned} \tag{C.6}$$

$$\begin{aligned}\left[\boldsymbol{\nu}\times\left(\mu^{-1}\nabla\times\mathbf{E}\right)\right]_{\Gamma_-} &= \boldsymbol{\nu}\times\left(\mu^{-1}\nabla\times\mathbf{E}^{\delta}\right)\Big|_{\Gamma_-} - \boldsymbol{\nu}\times\left(\mu^{-1}\nabla\times\mathbf{E}^{out}\right)\Big|_{\Gamma_-}\\ &= \boldsymbol{\nu}\times\left(\mu^{-1}\nabla\times\mathbf{E}^{\delta}\right)\Big|_{\Gamma_-},\end{aligned} \tag{C.7}$$

$$\left[\mathbf{n}\times\left(\mu^{-1}\nabla\times\mathbf{E}\right)\right]_{\mathscr{S}} = -\mathbf{n}\times\left(\mu^{-1}\nabla\times\mathbf{E}^{\delta}\right)\Big|_{\mathscr{S}} \tag{C.8}$$

thus combining (C.1) and (C.2) with (C.3)–(C.8),

$$\begin{aligned}\boldsymbol{\nu}\times\mathbf{E}^{\delta}\Big|_{\Gamma_+} &= \mathrm{i}k\frac{\delta}{2}\overline{\boldsymbol{\xi}} + \mathrm{i}k(\boldsymbol{\nu}\times\overline{\boldsymbol{\eta}}),\\ \boldsymbol{\nu}\times\mathbf{E}^{\delta}\Big|_{\Gamma_-} &= -\mathrm{i}k\frac{\delta}{2}\overline{\boldsymbol{\xi}} + \mathrm{i}k(\boldsymbol{\nu}\times\overline{\boldsymbol{\eta}}),\\ \mathbf{n}\times\mathbf{E}^{\delta}\Big|_{\mathscr{S}} &= \mathrm{i}k(\mathbf{n}\times\overline{\boldsymbol{\sigma}}),\end{aligned}$$

and

$$\begin{aligned}\boldsymbol{\nu}\times\left(\mu^{-1}\nabla\times\mathbf{E}^{\delta}\right)\Big|_{\Gamma_+} &= -\mathrm{i}k(\boldsymbol{\nu}\times\overline{\mathcal{A}_1}^{-1}\overline{\boldsymbol{\xi}}) - \mathrm{i}k\frac{\delta}{2}\overline{\mathcal{A}_2}\overline{\boldsymbol{\eta}},\\ \boldsymbol{\nu}\times\left(\mu^{-1}\nabla\times\mathbf{E}^{\delta}\right)\Big|_{\Gamma_-} &= -\mathrm{i}k(\boldsymbol{\nu}\times\overline{\mathcal{A}_1}^{-1}\overline{\boldsymbol{\xi}}) + \mathrm{i}k\frac{\delta}{2}\overline{\mathcal{A}_2}\overline{\boldsymbol{\eta}},\\ \mathbf{n}\times\left(\mu^{-1}\nabla\times\mathbf{E}^{\delta}\right)\Big|_{\mathscr{S}} &= \mathbf{0}.\end{aligned}$$

Introducing the following notation for the *internal jump* and the *internal mean value*

$$[\![u^{\delta}]\!]_{\Omega_\delta} := u^{\delta}\Big|_{\Gamma_+} - u^{\delta}\Big|_{\Gamma_-}, \quad \langle\!\langle u^{\delta}\rangle\!\rangle_{\Omega_\delta} := \frac{1}{2}(u^{\delta}\Big|_{\Gamma_+} + u^{\delta}\Big|_{\Gamma_-})$$

for every u^{δ} (scalar or vectorial field) defined in Ω_δ, we know that,

$$[\![\boldsymbol{\nu}\times\mathbf{E}^{\delta}]\!]_{\Omega_\delta} = \mathrm{i}k\delta\overline{\boldsymbol{\xi}}, \qquad \langle\!\langle\mathbf{E}^{\delta}_T\rangle\!\rangle_{\Omega_\delta} = \mathrm{i}k\overline{\boldsymbol{\eta}},$$

and

$$[\![\boldsymbol{\nu}\times\left(\mu^{-1}\nabla\times\mathbf{E}^{\delta}\right)]\!]_{\Omega_\delta} = -\mathrm{i}k\delta\overline{\mathcal{A}_2}\overline{\boldsymbol{\eta}}, \qquad \langle\!\langle(\mu^{-1}\nabla\times\mathbf{E}^{\delta})_T\rangle\!\rangle_{\Omega_\delta} = -\mathrm{i}k\overline{\mathcal{A}_1}^{-1}\overline{\boldsymbol{\xi}}.$$

Therefore, $\mathbf{E}^{\delta} = \mathbf{E}|_{\Omega_\delta} \in \mathbf{H}(\mathrm{curl},\Omega_\delta)$ satisfies

$$\nabla\times\mu_{\pm}^{-1}\nabla\times\mathbf{E}^{\delta} - k^2\epsilon_{\pm}\mathbf{E} = \mathbf{0} \quad \text{in} \quad \Omega_\delta^{\pm}, \tag{C.9}$$

$$\overline{\mathcal{A}_1}^{-1}[\![\boldsymbol{\nu}\times\mathbf{E}^{\delta}]\!]_{\Omega_\delta} = -\delta\langle\!\langle(\mu^{-1}\nabla\times\mathbf{E}^{\delta})_T\rangle\!\rangle_{\Omega_\delta}, \tag{C.10}$$

$$[\![\boldsymbol{\nu}\times\left(\mu^{-1}\nabla\times\mathbf{E}^{\delta}\right)]\!]_{\Omega_\delta} = -\delta\overline{\mathcal{A}_2}\langle\!\langle\mathbf{E}^{\delta}_T\rangle\!\rangle_{\Omega_\delta}, \tag{C.11}$$

$$\mathbf{n}\times\left(\mu^{-1}\nabla\times\mathbf{E}^{\delta}\right)\Big|_{\mathscr{S}} = \mathbf{0}, \qquad \text{and} \qquad \mathbf{n}\times\mathbf{E}^{\delta}\Big|_{\mathscr{S}} = \mathrm{i}k(\mathbf{n}\times\overline{\boldsymbol{\sigma}}). \tag{C.12}$$

Notice that (C.9)–(C.12) is an over-determined system which in general may not have a solution. However, to investigate it further, we multiply by a test function and integrate by parts we have that $\mathbf{E}^\delta$ necessarily satisfies

$$a_{\Omega_\delta}(\mathbf{E}^\delta, \mathbf{v}^\delta) = 0, \quad \text{for all} \quad \mathbf{v}^\delta \in \mathcal{H}_0^\delta, \tag{C.13}$$

where

$$\begin{aligned} a_{\Omega_\delta}(\mathbf{E}^\delta, \mathbf{v}^\delta) = &\int_{\Omega_\delta} \left\{ \mu_\pm^{-1} \nabla \times \mathbf{E}^\delta \cdot \nabla \times \overline{\mathbf{v}}^\delta - k^2 \epsilon_\pm \mathbf{E}^\delta \cdot \overline{\mathbf{v}}^\delta \right\} \, \mathrm{d}\mathbf{y} \\ &+ \frac{1}{\delta} \int_{\Gamma_0} \overline{\mathcal{A}_1}^{-1} [\![\boldsymbol{\nu} \times \mathbf{E}^\delta]\!]_{\Omega_\delta} \cdot [\![\boldsymbol{\nu} \times \overline{\mathbf{v}}^\delta]\!]_{\Omega_\delta} \, \mathrm{d}s(\mathbf{y}) \\ &- \int_{\Gamma_0} \delta \overline{\mathcal{A}_2} \langle\!\langle \mathbf{E}_T^\delta \rangle\!\rangle_{\Omega_\delta} \cdot \langle\!\langle \overline{\mathbf{v}}^\delta \rangle\!\rangle_{\Omega_\delta} \, \mathrm{d}s(\mathbf{y}), \end{aligned}$$

and

$$\mathcal{H}_0^\delta = \left\{ \mathbf{u}^\delta \in \mathbf{H}(\mathrm{curl}, \Omega_\delta) \,\middle|\, \langle\!\langle \mathbf{u}_T^\delta \rangle\!\rangle_{\Omega_\delta} \in \mathbf{H}(\mathrm{curl}_\Gamma, \Gamma_0) \ \text{ and } \ \mathbf{n} \times \left(\mu^{-1} \nabla \times \mathbf{u}^\delta \right) \Big|_{\mathscr{S}} = \mathbf{0} \right\},$$

equipped with the graph norm

$$\left\| \mathbf{u}^\delta \right\|_{\mathcal{H}_0^\delta}^2 = \left\| \mathbf{u}^\delta \right\|_{\mathbf{H}(\mathrm{curl}, \Omega_\delta)}^2 + \left\| \langle\!\langle \mathbf{u}_T^\delta \rangle\!\rangle_{\Omega_\delta} \right\|_{\mathbf{H}(\mathrm{curl}_\Gamma, \Gamma_0)}^2 .$$

Observe now that $a_{\Omega_\delta}(\cdot, \cdot)$ has the same structure as the sesquilinear form $a^+(\cdot, \cdot) + b(\cdot, \cdot)$, where $a^+(\cdot, \cdot)$ and $b(\cdot, \cdot)$ are respectively defined in (15) and (16). Notice that the real parts appearing in the boundary integrals remain the same, and only the imaginary parts invert signs. It is important to observe that since the Calderón map G_e does not play a role in this interior problem (C.13), then the sign of the imaginary part is not important, as long as it is non-zero, just as in the case we are considering. Therefore, repeating essentially the same arguments given in the proof of theorem 2.1, it is possible to prove that the problem (C.13) is well posed under the same assumptions on the material properties.

Therefore, the unique solution to (C.13) is $\mathbf{E}^\delta = \mathbf{0}$. We then deduce that $(\boldsymbol{\xi}, \boldsymbol{\eta}, \boldsymbol{\sigma}) = (\mathbf{0}, \mathbf{0}, \mathbf{0})$, and thus $\mathscr{H}^*$ is injective, implying that $\mathscr{H}$ has dense range.

Now, to show that $\mathscr{H}$ is injective, lets observe that if $\mathscr{H}(\mathbf{g}) = \mathbf{0}$, then in particular $\mathbf{n} \times (\mu^{-1} \nabla \times \mathbf{E}_{b,\mathbf{g}}) \Big|_{\mathscr{S}} = \mathbf{0}$, which by the assumption is only possible if $\mathbf{g} = \mathbf{0}$. □

ORCID iDs

Fioralba Cakoni https://orcid.org/0000-0002-4648-8780
Irene de Teresa https://orcid.org/0000-0002-4691-9501

References

[1] Ammari H and Kang H 2004 *Reconstruction of Small Inhomogeneities from Boundary Measurements* (*Lecture Notes in Mathematics* vol 1846) (Berlin: Springer)
[2] Ammari H, Kang H and Santosa F 2006 Scattering of electromagnetic waves by thin dielectric planar structures *SIAM J. Math. Anal.* **38** 1329–42
[3] Assous F and Michaeli M 2011 Solving Maxwell's equations in singular domains with Nitsche type method *J. Comput. Phys.* **230** 4922–39

[4] Audibert L, Girard A and Haddar H 2015 Identifying defects in an unknown background using differential measurements *Inverse Problems Imaging* **9** 625–43
[5] Bondarenko O, Kirsch A and Liu X 2013 The factorization method for inverse acoustic scattering in a layered medium *Inverse Problems* **29** 045010
[6] Cakoni F, Colton D and Monk P 2011 *The Linear Sampling Method in Inverse Electromagnetic Scattering* (*CBMS-NSF Regional Conf. Series in Applied Mathematics* vol 80) (Philadelphia, PA: SIAM)
[7] Cakoni F, de Teresa I, Haddar H and Monk P 2016 Nondestructive testing of the delaminated interface between two materials *SIAM J. Appl. Math.* **76** 2306–32
[8] Cakoni F and Harris I 2015 The factorization method for a defective region in an anisotropic material *Inverse Problems* **31** 025002
[9] Chun S, Haddar H and Hesthaven J 2010 High-order accurate thin layer approximations for time-domain electromagnetics, Part II: transmission layers *J. Comput. Appl. Math.* **234** 2587–608
[10] Colton D and Kress R 2013 *Inverse Acoustic and Electromagnetic Scattering Theory* 3rd edn (New York: Springer)
[11] de Teresa I 2017 Asymptotic methods in inverse scattering for inhomogeneous media *PhD Thesis* University of Delaware (http://udspace.udel.edu/handle/19716/23028)
[12] de Teresa I and Pourahmadian F Active imaging of interfacial damage in layered composites to appear
[13] Delourme B, Haddar H and Joly P 2013 On the well-posedness, stability and accuracy of an asymptotic model for thin periodic interfaces in electromagnetic scattering problems *Math. Models Methods Appl. Sci.* **23** 2433–64
[14] Deng Y and Liu X 2011 Electromagnetic imaging methods for nondestructive evaluation applications *Sensors* **11** 11774–808
[15] do Carmo M P 1976 *Differential Geometry of Curves and Surfaces* 2nd edn (New Jersey: Prentice-Hall)
[16] Durufle M, Péron V and Poignard C 2014 Thin layer models for electromagnetism *Commun. Comput. Phys.* **16** 213–38
[17] Franchois A and Pichot C 1997 Microwave imaging-complex permittivity reconstruction with a Levenberg–Marquardt method *IEEE Trans. Antennas Propag.* **45** 203–15
[18] Haddar H and Joly P 2002 Stability of thin layer approximation of electromagnetic waves scattering by linear and nonlinear coatings *J. Comput. Appl. Math.* **143** 201–36
[19] Kharkovsky S and Zoughi R 2007 Microwave and millimeter wave nondestructive testing and evaluation—overview and recent advances *IEEE Instrum. Meas. Mag.* **10** 26–38
[20] McLean W 2000 *Strongly Elliptic Systems and Boundary Integral Equations* (Cambridge: Cambridge University Press)
[21] Monk P 2003 *Finite Element Methods for Maxwell's Equations* (Oxford: Oxford University Press)
[22] Nédélec J 2000 *Acoustic and Electromagnetic Equations* (New York: Springer)
[23] Nitsche J 1971 Über ein Variationsprinzip zur Lösung von Dirichlet-Problemen bei Verwendung von Teilräumen, die keinen Randbedingungen unterworfen sind *Abh. Math. Semin. Univ. Hamburg* **36** 9–15
[24] Ōkaji T 2002 Strong unique continuation property for time harmonic Maxwell equations *J. Math. Soc. Japan* **54** 89–122
[25] Özdemir Ö, Haddar H and Yaka A 2011 Reconstruction of the electromagnetic field in layered media using the concept of approximate transmission conditions *IEEE Trans. Antennas Propag.* **59** 2964–72
[26] Potthast R 1998 A point-source method for inverse acoustic and electromagnetic obstacle scattering problems *IMA J. Appl. Math.* **61** 119–40
[27] Pourahmadian F, Guzina B and Haddar H 2017 A synoptic approach to the seismic sensing of heterogeneous fractures: from geometric reconstruction to interfacial characterization *Comput. Methods Appl. Mech. Eng.* **324** 395–412
[28] Schöberl J 2017 Netgen/NGSolve https://ngsolve.org
[29] Tamori Y, Suzuki E and Deng W M 2016 Epithelial tumors originate in tumor hotspots, a tissue-intrinsic microenvironment *PLoS Biol.* **14** e1002537
[30] Zeev N and Cakoni F 2009 The identification of thin dielectric objects from far field or near field scattering data *SIAM J. Appl. Math.* **69** 1024–42